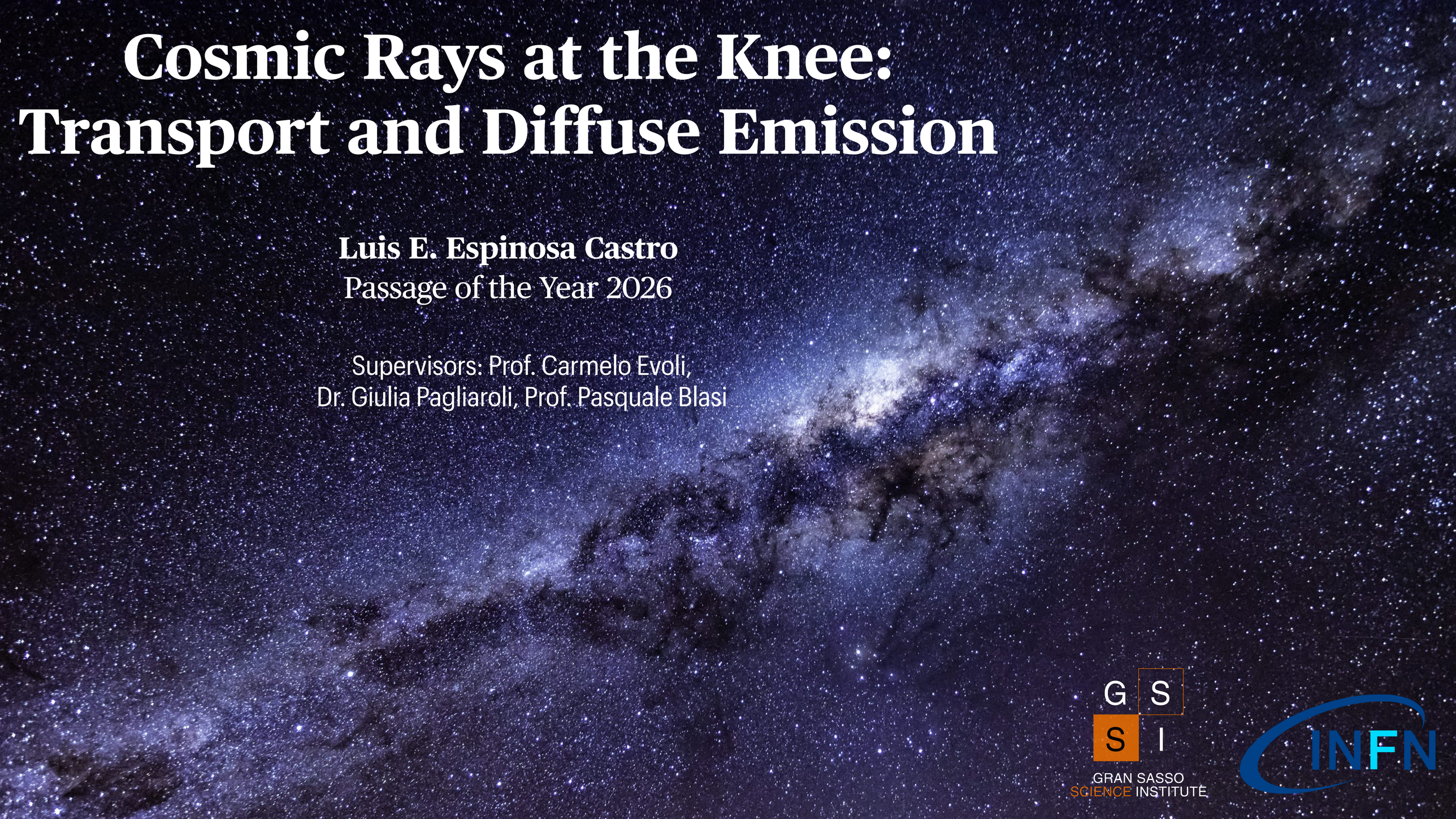
Cosmic Rays at the Knee: Transport and Diffuse Emission

Luis E. Espinosa Castro
Passage of the Year 2026

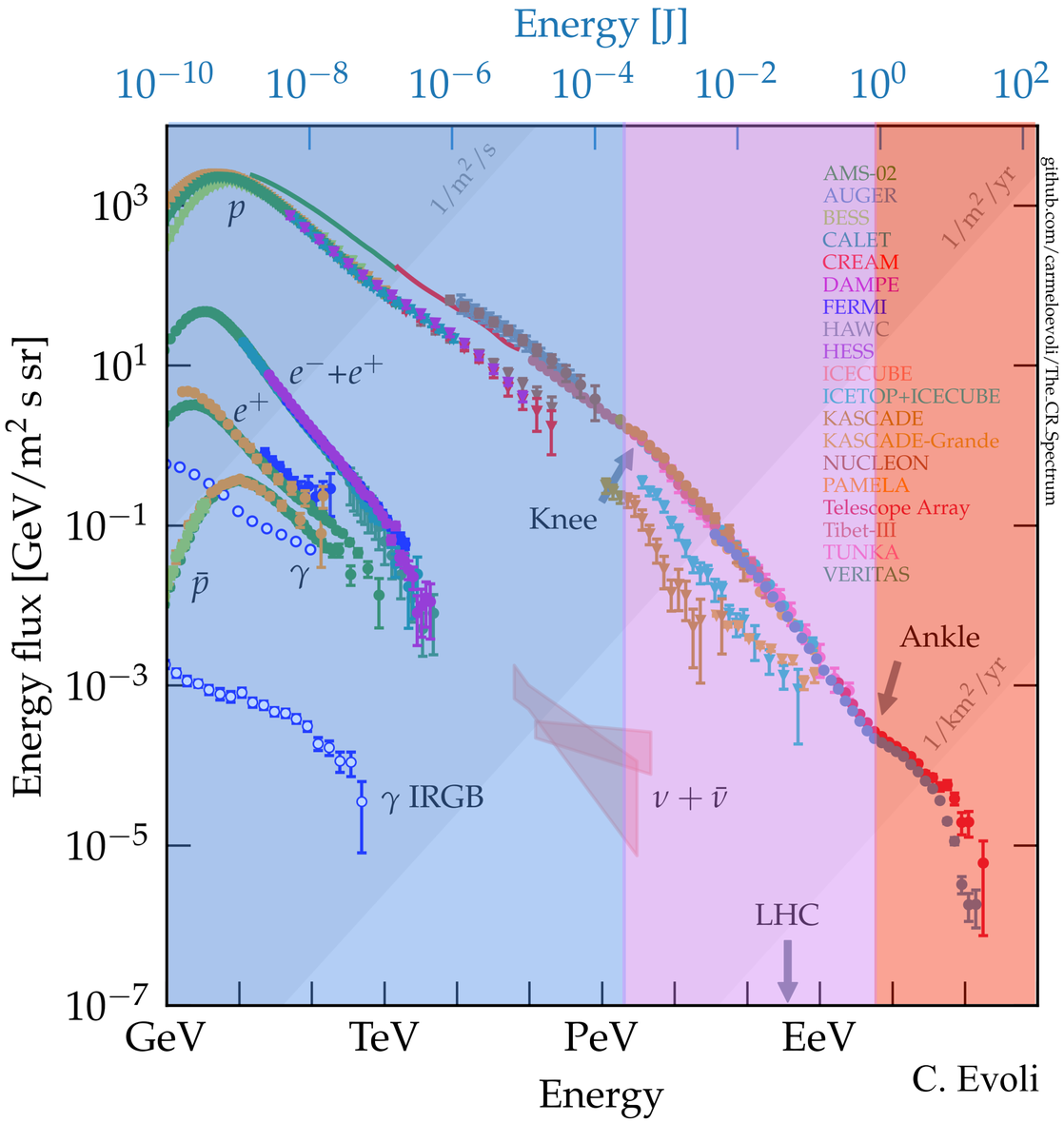
Supervisors: Prof. Carmelo Evoli,
Dr. Giulia Pagliaroli, Prof. Pasquale Blasi



The Cosmic Ray Spectrum

GeV - PeV energy cosmic rays are associated to **Galactic** sources while cosmic rays above the ankle are thought to be of **extragalactic** origin.

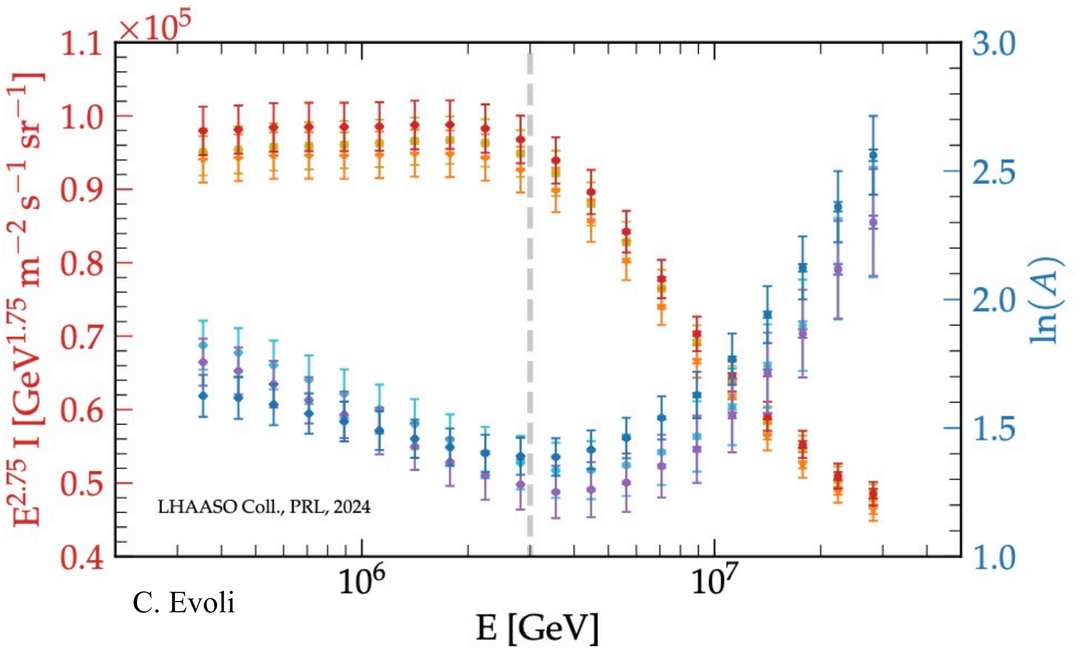
- What happens in the **transition regime**?
- Are there additional cosmic ray population(s) in this energy range?
- What can we learn about the Galactic environment or sources?
- Is the **knee** linked to the maximum energy of the Galactic cosmic ray population? What is the origin of this feature?



The Cosmic Ray Knee

What we know:

- Break located at 3.67 ± 0.15 PeV in the all-particle spectrum.
- Feature compatible with change in composition, measured by $\langle \ln A \rangle$.

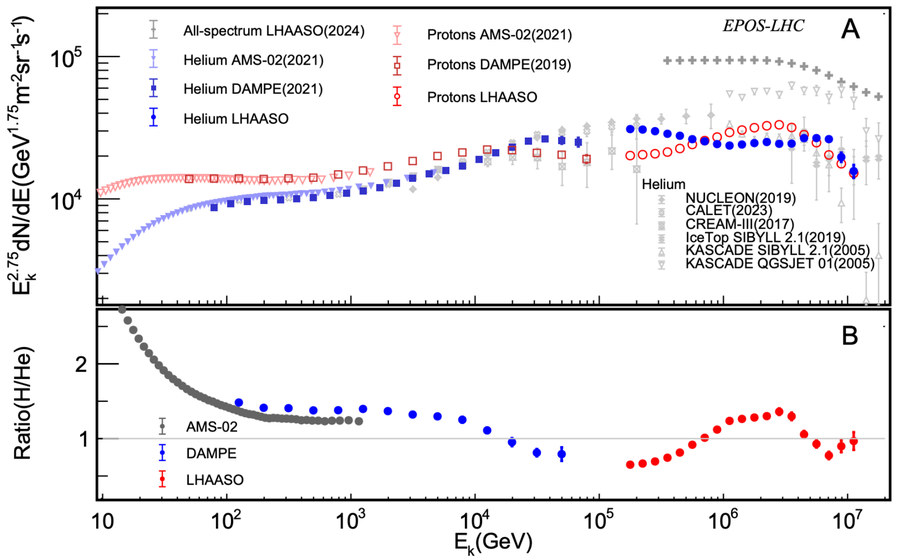


The Cosmic Ray Knee

What we know:

- Break located at 3.67 ± 0.15 PeV in the all-particle spectrum.
- Feature compatible with change in composition, measured by $\langle \ln A \rangle$.
- Compatible with proton break (3.3 ± 0.5 PeV) and in good agreement with helium break at the same rigidity (~ 3.5 PV).

LHAASO Coll., PRL, 2026

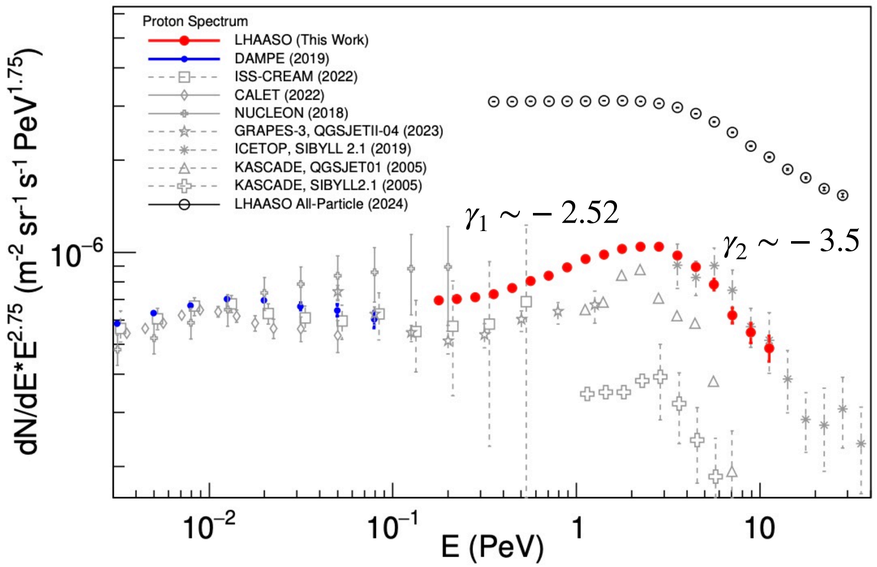


The Cosmic Ray Knee

What we know:

- Break located at 3.67 ± 0.15 PeV in the all-particle spectrum.
- Feature compatible with change in composition, measured by $\langle \ln A \rangle$.
- Compatible with proton break (3.3 ± 0.5 PeV) and in good agreement with helium break at the same rigidity (~ 3.5 PV).

LHAASO Coll., Sci. Bull., 2025

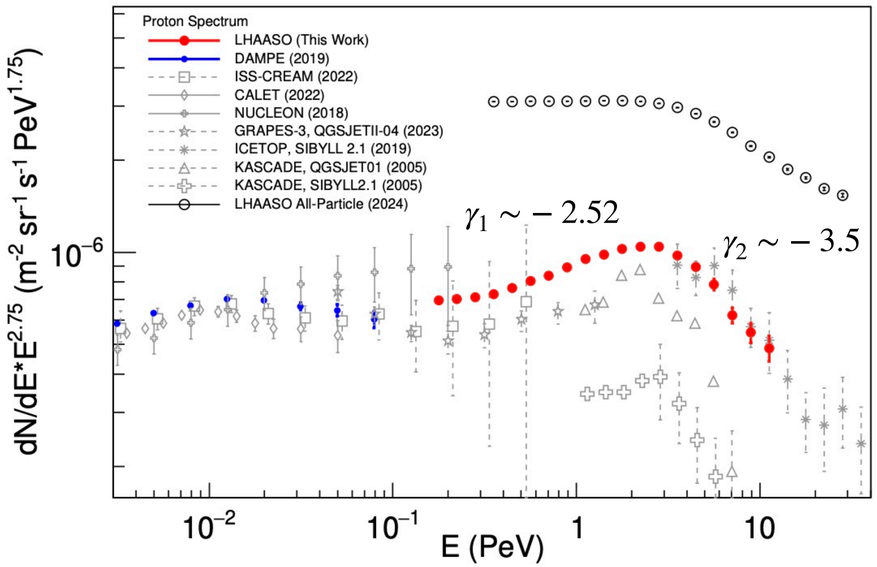


The Cosmic Ray Knee

What we know:

- Break located at 3.67 ± 0.15 PeV in the all-particle spectrum.
- Feature compatible with change in composition, measured by $\langle \ln A \rangle$.
- Compatible with proton break (3.3 ± 0.5 PeV) and in good agreement with helium break at the same rigidity (~ 3.5 PV).

LHAASO Coll., Sci. Bull., 2025



What we think:

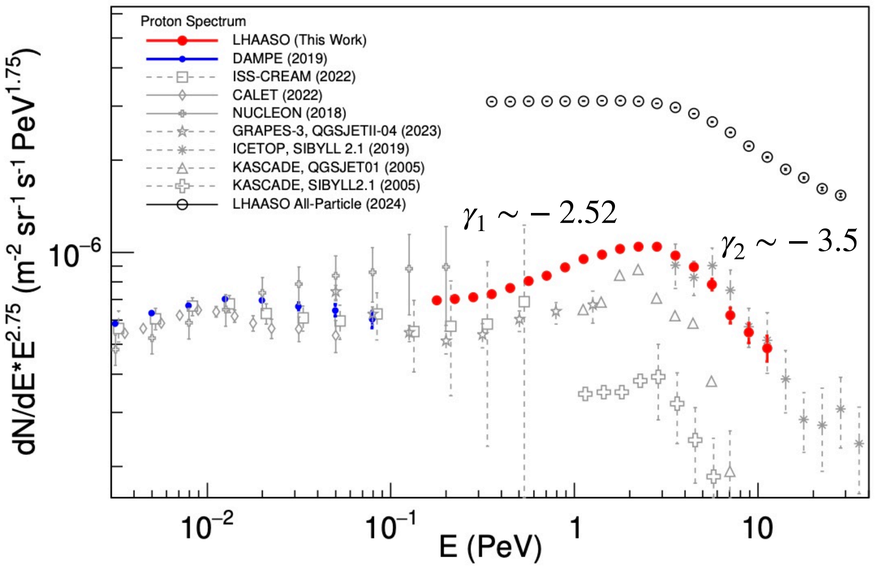
- Marks the maximum rigidity of the Galactic cosmic ray population.

The Cosmic Ray Knee

What we know:

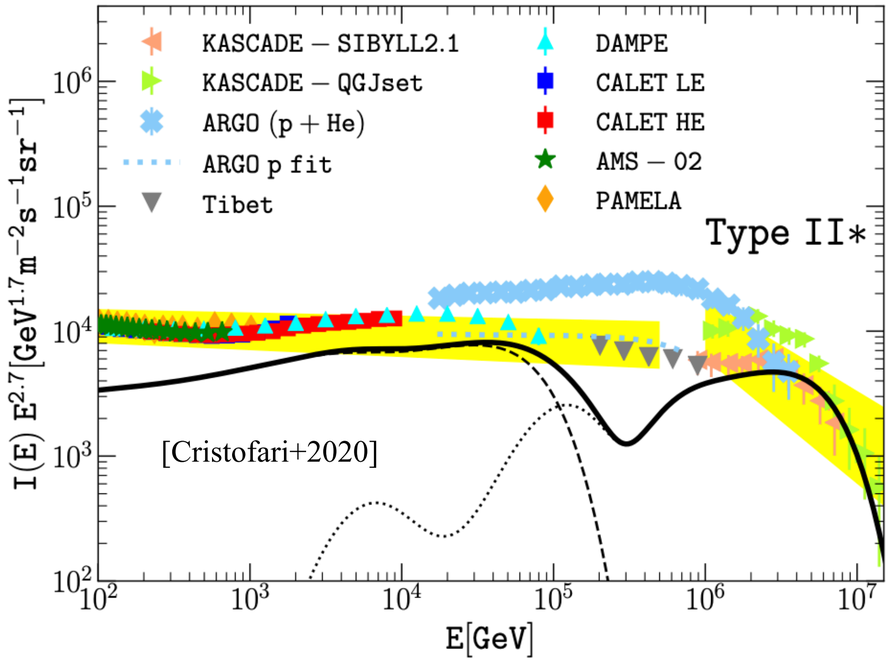
- Break located at 3.67 ± 0.15 PeV in the all-particle spectrum.
- Feature compatible with change in composition, measured by $\langle \ln A \rangle$.
- Compatible with proton break (3.3 ± 0.5 PeV) and in good agreement with helium break at the same rigidity (~ 3.5 PV).

LHAASO Coll., Sci. Bull., 2025



What we think:

- Marks the maximum rigidity of the Galactic cosmic ray population.
  - Imprint of the maximum energy achievable by Galactic accelerators (e.g. supernova remnants).

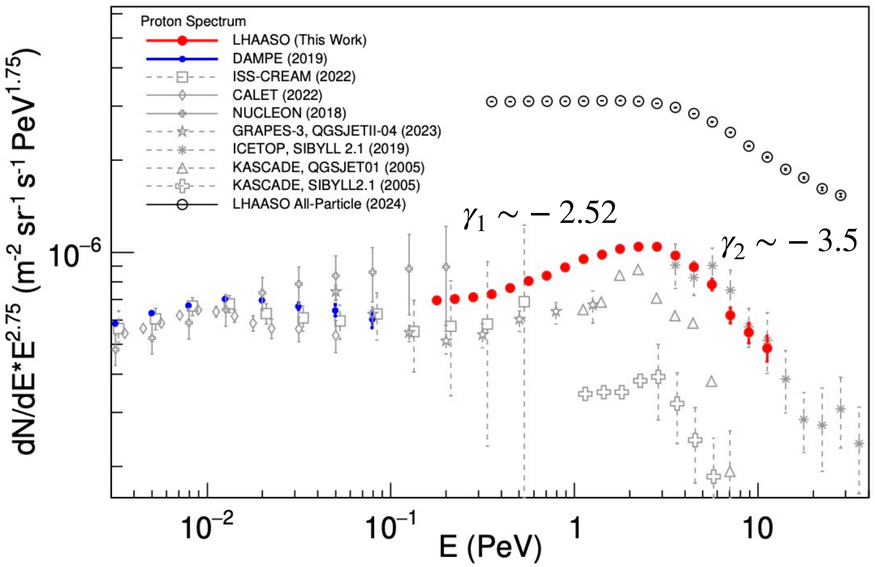


The Cosmic Ray Knee

What we know:

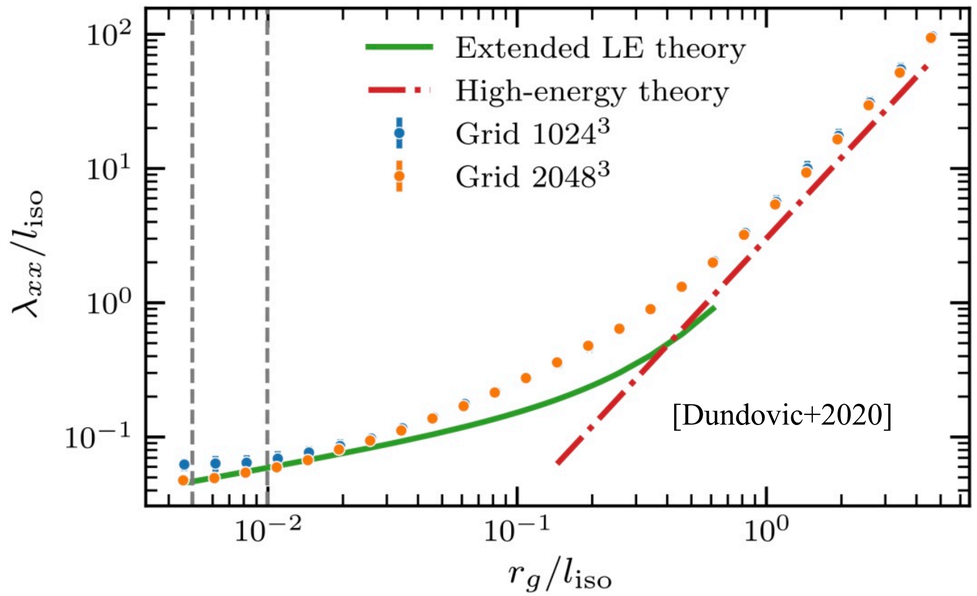
- Break located at 3.67 ± 0.15 PeV in the all-particle spectrum.
- Feature compatible with change in composition, measured by $\langle \ln A \rangle$.
- Compatible with proton break (3.3 ± 0.5 PeV) and in good agreement with helium break at the same rigidity (~ 3.5 PV).

LHAASO Coll., Sci. Bull., 2025



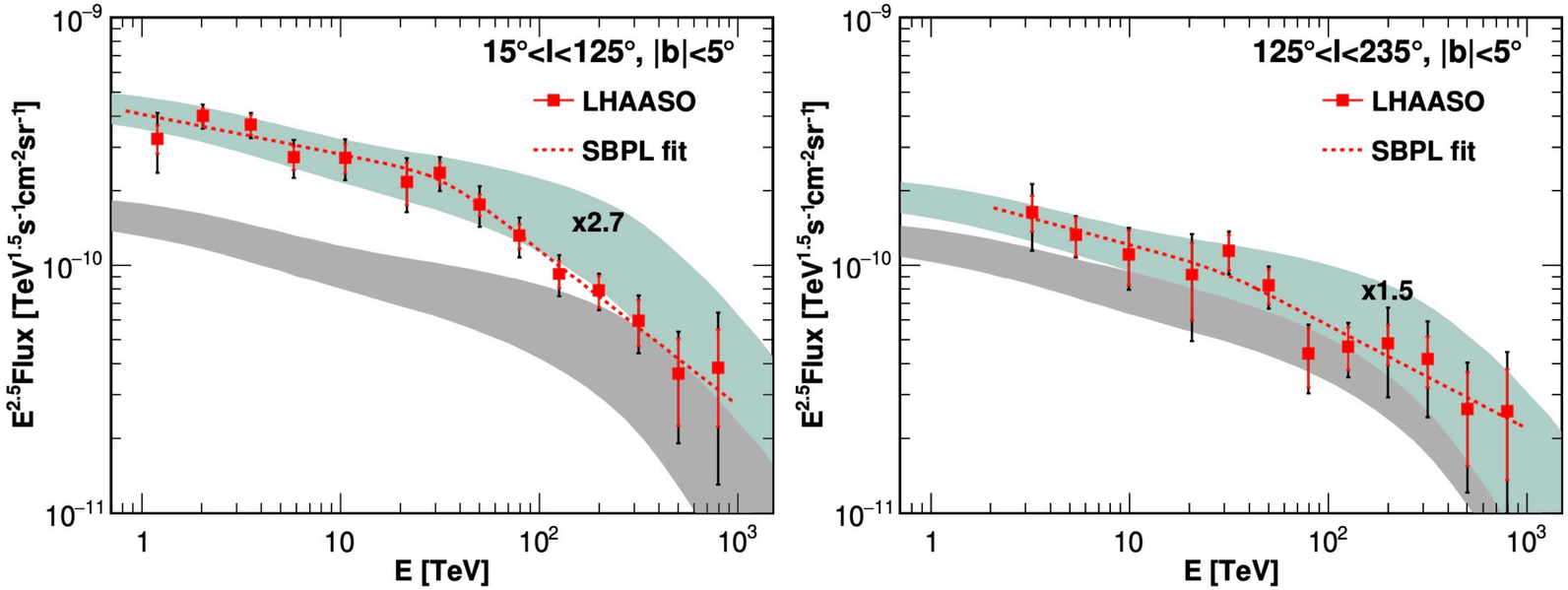
What we think:

- Marks the maximum rigidity of the Galactic cosmic ray population.
  - Imprint of the maximum energy achievable by Galactic accelerators (e.g. supernova remnants).
  - Caused by changes of the transport of cosmic rays in the Galactic turbulent magnetic field.

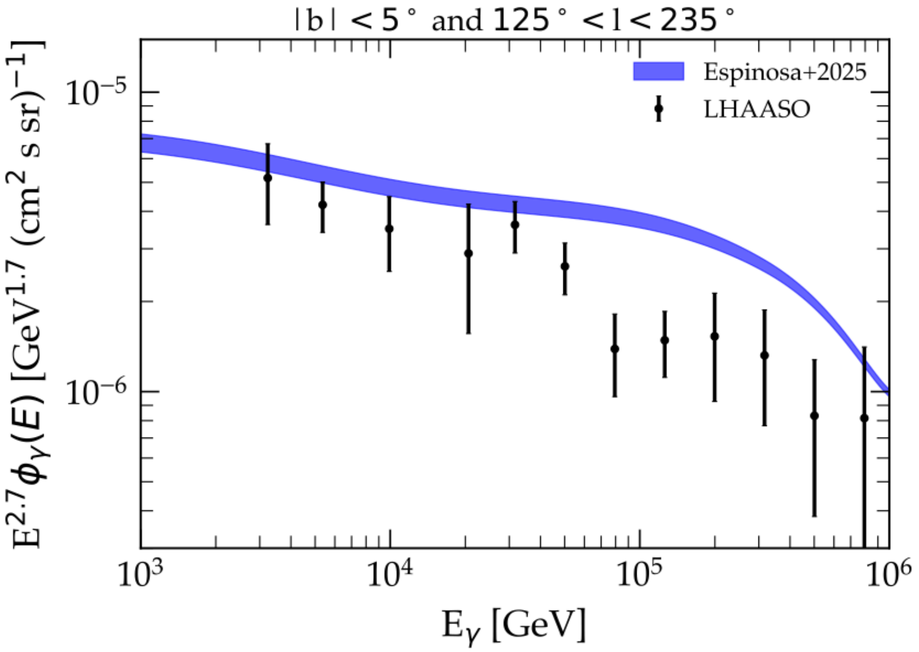


The ‘Source’ Scenario

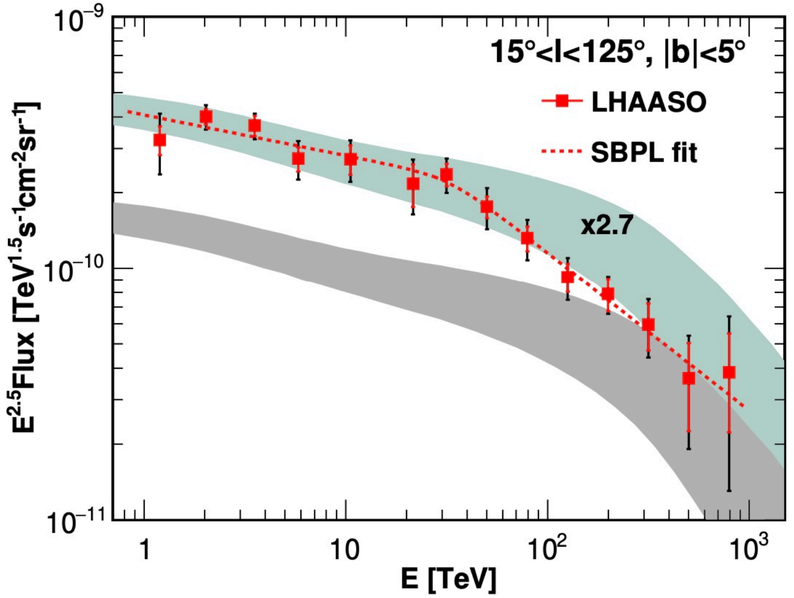
Diffuse gamma-ray flux measured by LHAASO in two Galaxy regions **[Cao+2025].**

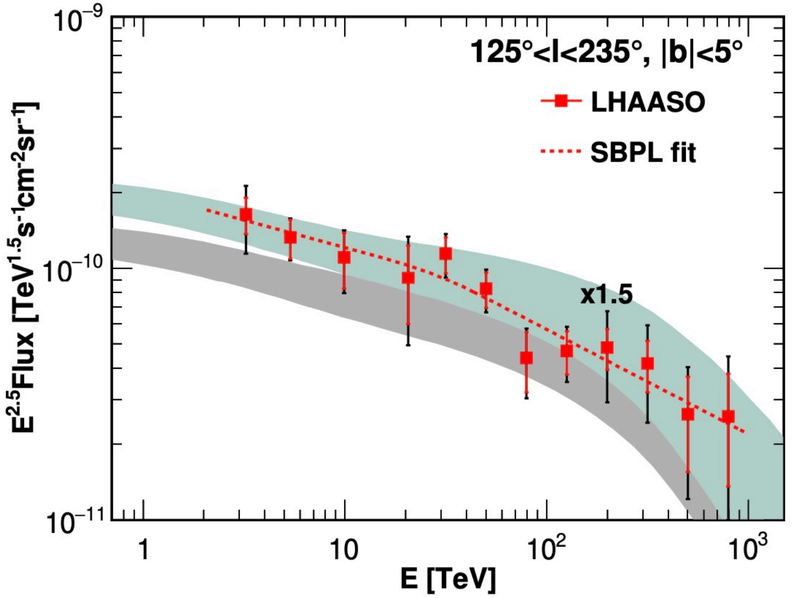


Spectral disagreement between observations and predicted diffuse gamma-ray emission based on LHAASO proton flux **[Espinosa+2025]**.

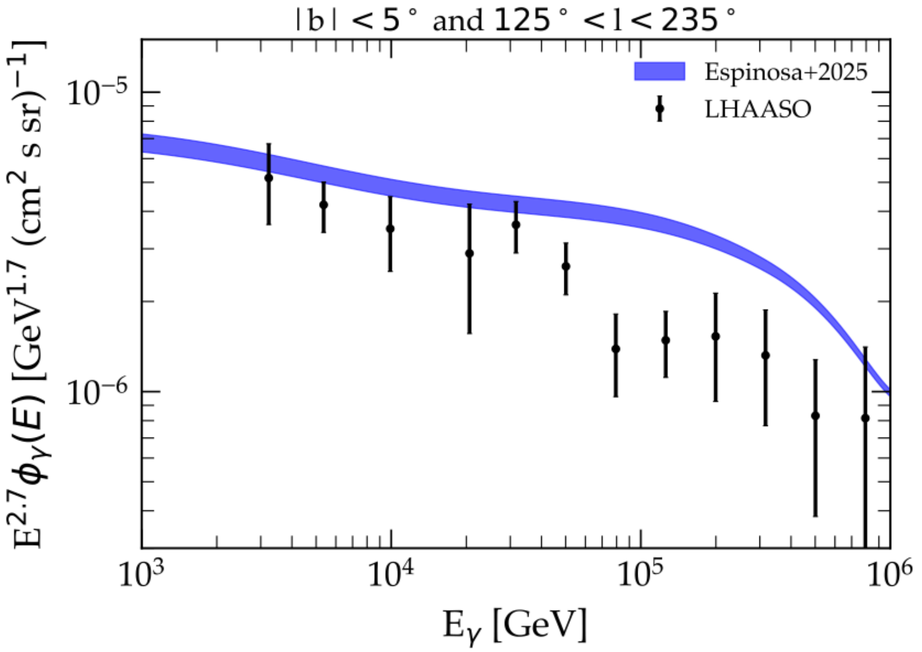


Diffuse gamma-ray flux measured by LHAASO in two Galaxy regions **[Cao+2025].**





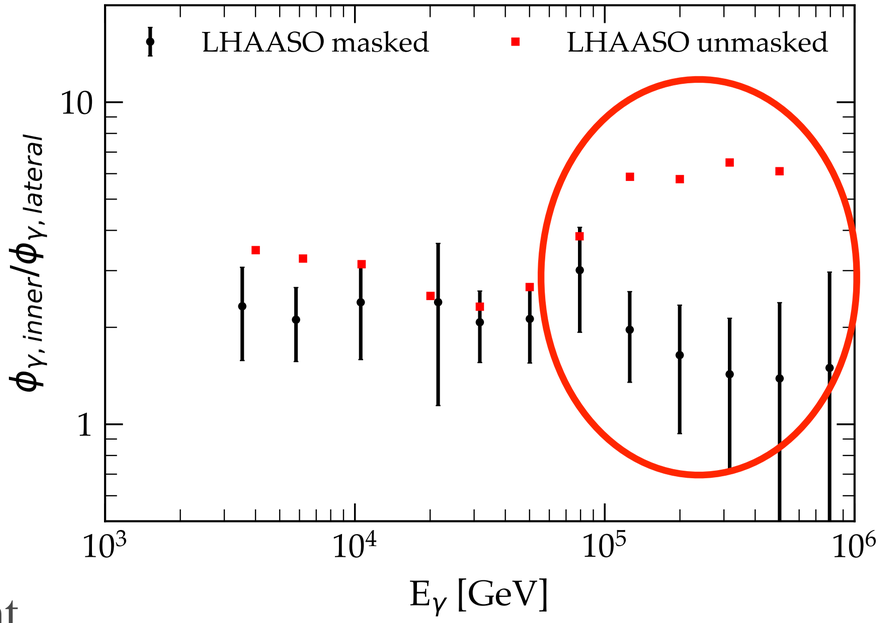
Spectral disagreement between observations and predicted diffuse gamma-ray emission based on LHAASO proton flux **[Espinosa+2025]**.

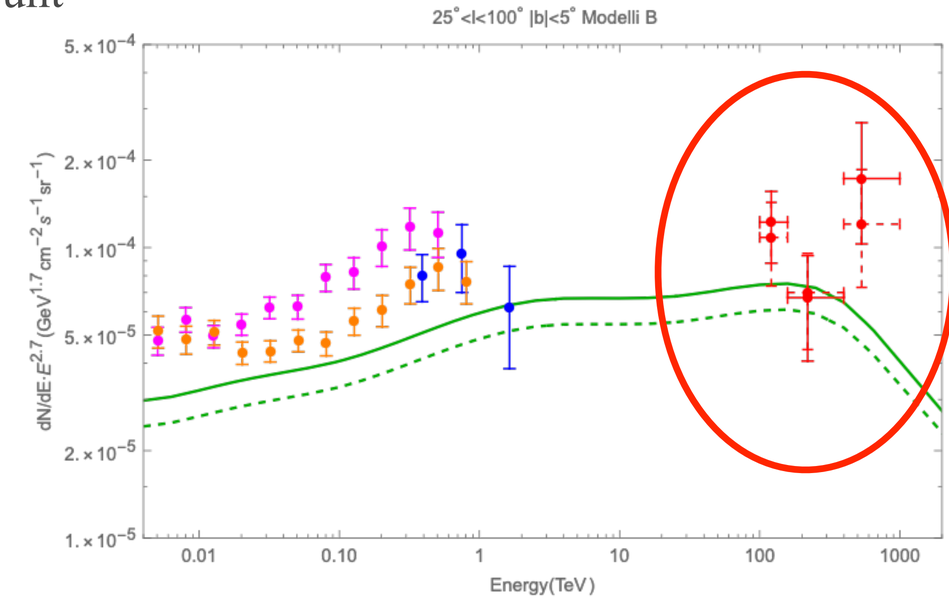


Gamma-ray excess found in inner Galactic region from LHAASO but no similar excess found in Tibet ASγ data.

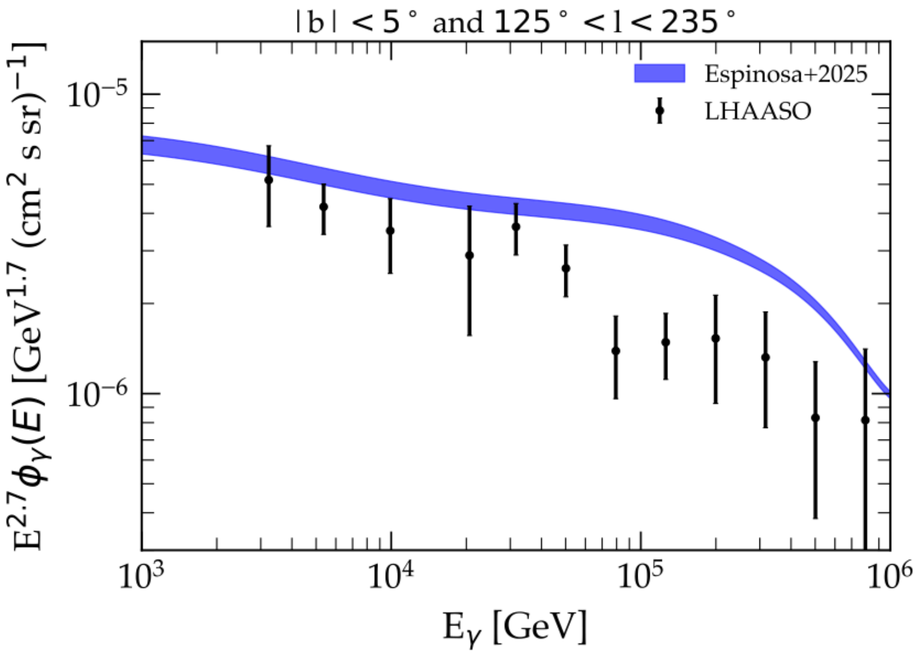
LHAASO: $15° < l < 125°$
$125° < l < 235°$
Tibet ASγ: $25° < l < 100°$
$50° < l < 200°$

A high-energy component in region in common could account for this.





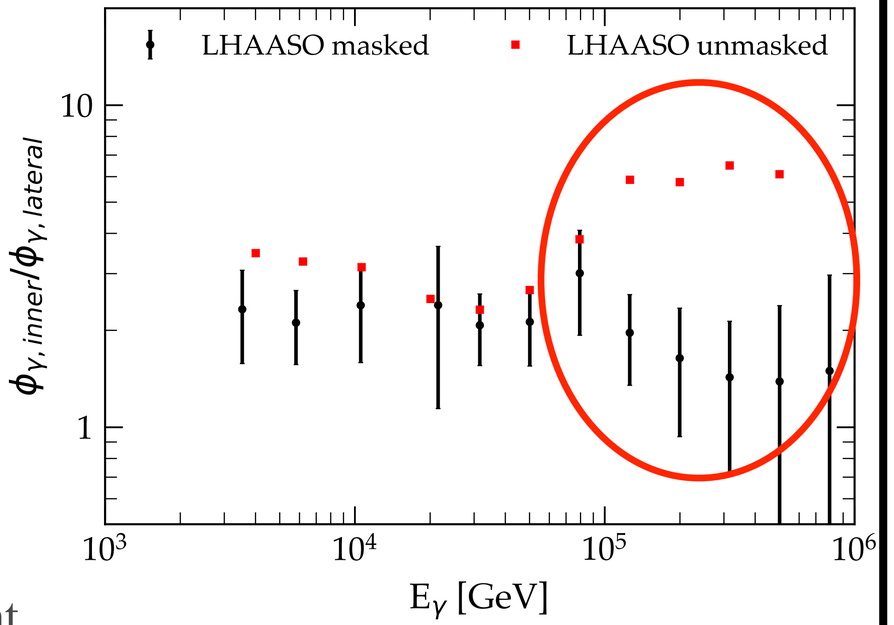
Spectral disagreement between observations and predicted diffuse gamma-ray emission based on LHAASO proton flux **[Espinosa+2025]**.



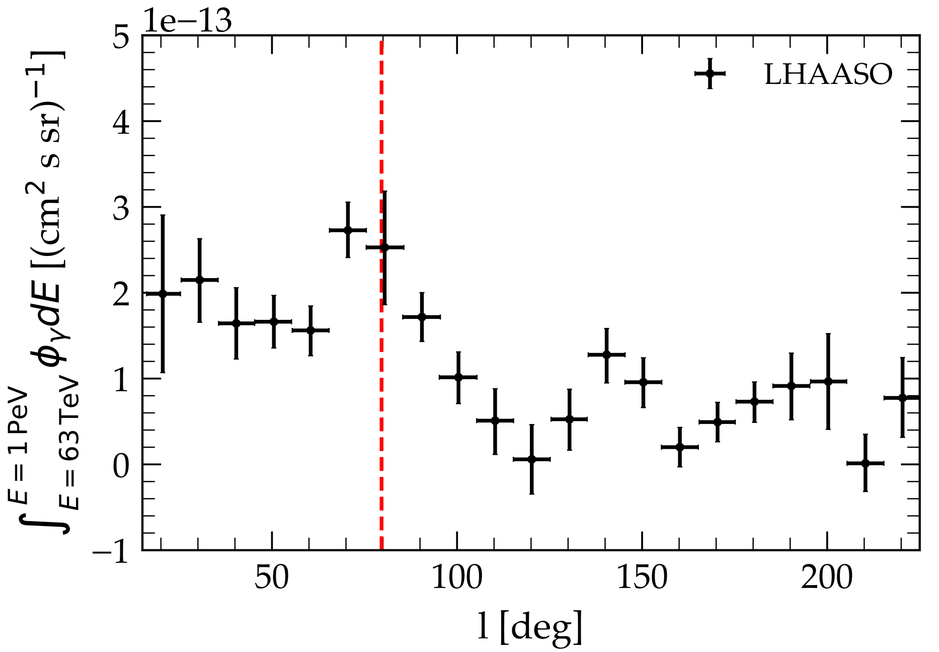
Gamma-ray excess found in inner Galactic region from LHAASO but no similar excess found in Tibet ASγ data.

LHAASO:	$15° < l < 125°$
	$125° < l < 235°$
Tibet ASγ:	$25° < l < 100°$
	$50° < l < 200°$

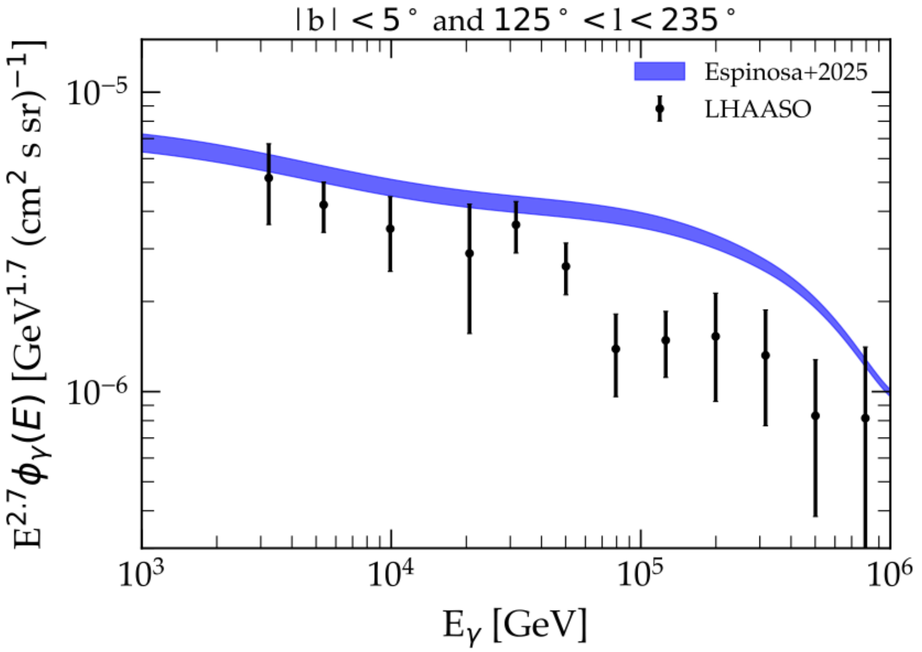
A high-energy component in region in common could account for this.



Compatible with longitudinal profile of diffuse gamma-rays at the highest energies.



Spectral disagreement between observations and predicted diffuse gamma-ray emission based on LHAASO proton flux **[Espinosa+2025]**.

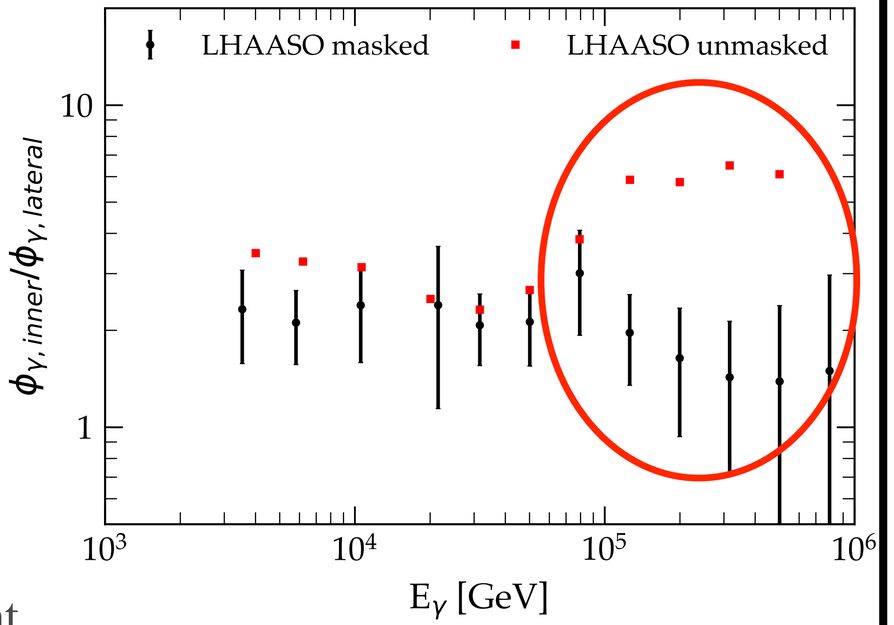


These spectral, spatial and multi-messenger evidence can be linked to a local source located in the **Cygnus region**

Gamma-ray excess found in inner Galactic region from LHAASO but no similar excess found in Tibet ASγ data.

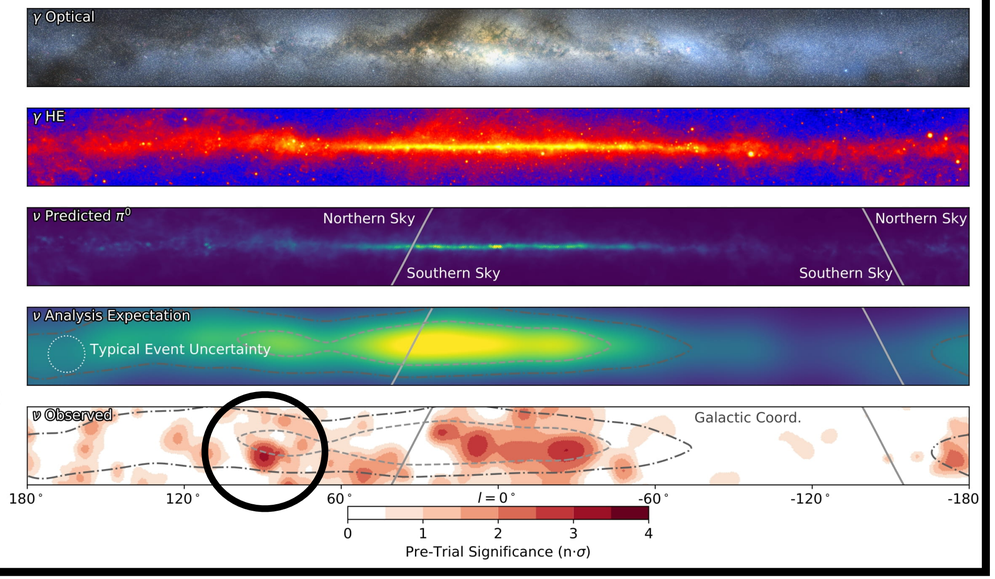
LHAASO:	$15° < l < 125°$
	$125° < l < 235°$
Tibet ASγ:	$25° < l < 100°$
	$50° < l < 200°$

A high-energy component in region in common could account for this.



Compatible with longitudinal profile of diffuse gamma-rays at the highest energies.

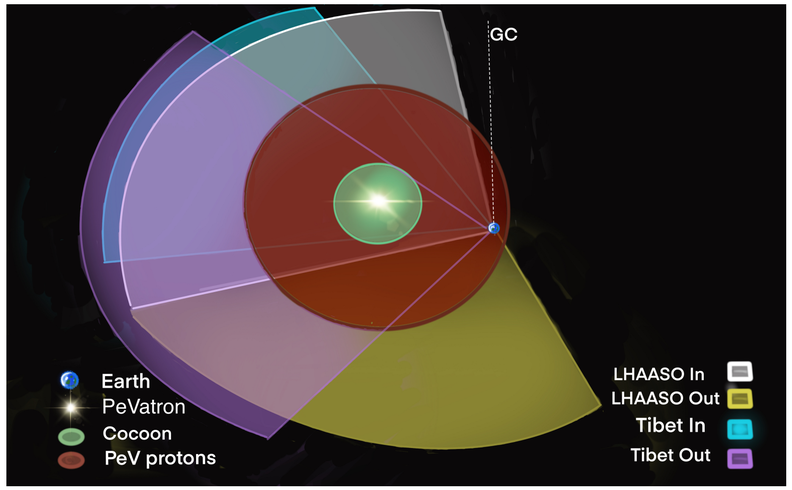
Neutrino observations along Galactic Plane by IceCube also show a slightly higher-significance in the same sky region.



Local Source Model

Cygnus continuous injection of protons following reported source parameters by LHAASO **[LHAASO Coll., 2024]**.

$$\dot{Q}(E_p) = \dot{Q}_0 \left(\frac{E_p}{E_0}\right)^{-s} \exp\left(-\frac{E_p}{E_p^{\max}}\right)$$



$R = 1.4\,\mathrm{kpc}, \quad E_{\max} = 6\,\mathrm{PeV},$

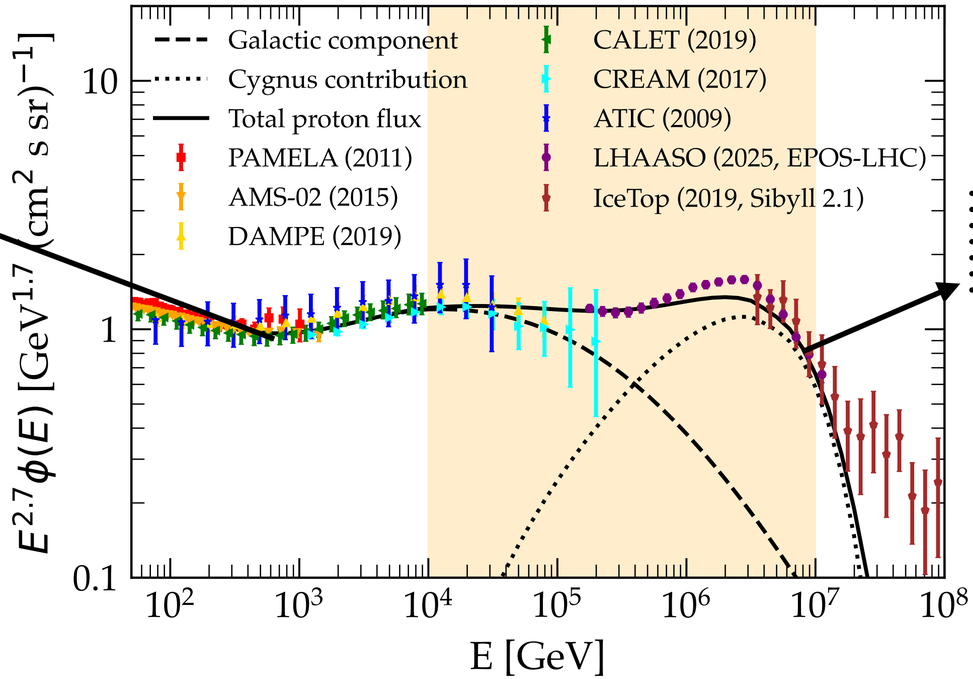
$s = 2.1, \quad L_p = \int dE_p\, E_p Q(E_p) = 3 \times 10^{37}\,\mathrm{erg\,s^{-1}}$

A two-zone diffusion model is adopted to solve the transport equation and estimate the flux of cosmic rays at Earth.

$$D(r, E_p) = \begin{cases} D_0 (E_p/E_0)^{\delta_0} & 0 < r < r_c, \\ D_1 (E_p/E_0)^{\delta_1} & r \geq r_c, \end{cases}$$

$$\frac{\partial n}{\partial t} = \frac{1}{r^2}\frac{\partial}{\partial r}\left(Dr^2 \frac{\partial n}{\partial r}\right) + Q$$

‘Cosmic ray sea’



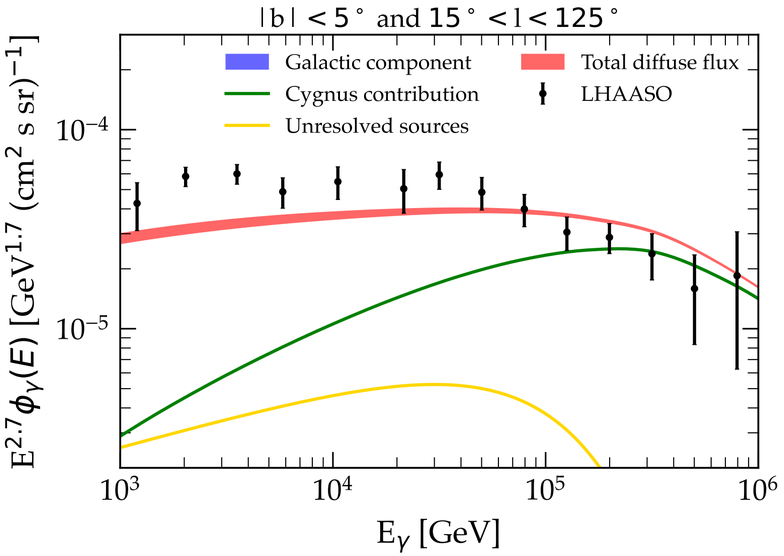
‘PeVatron island’

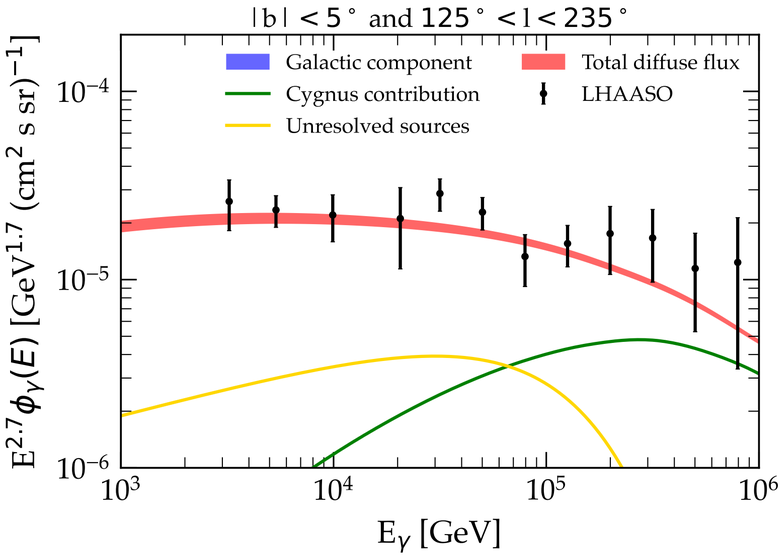
Results and Outlook

Inner Galaxy

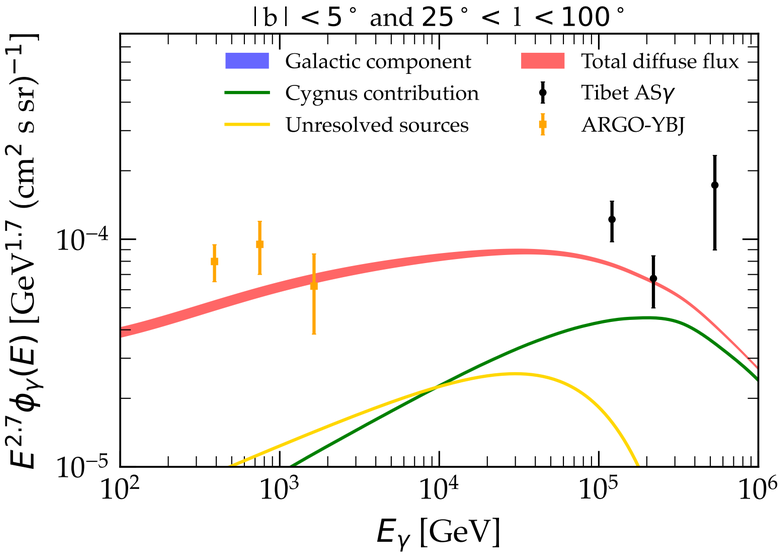
Outer Galaxy

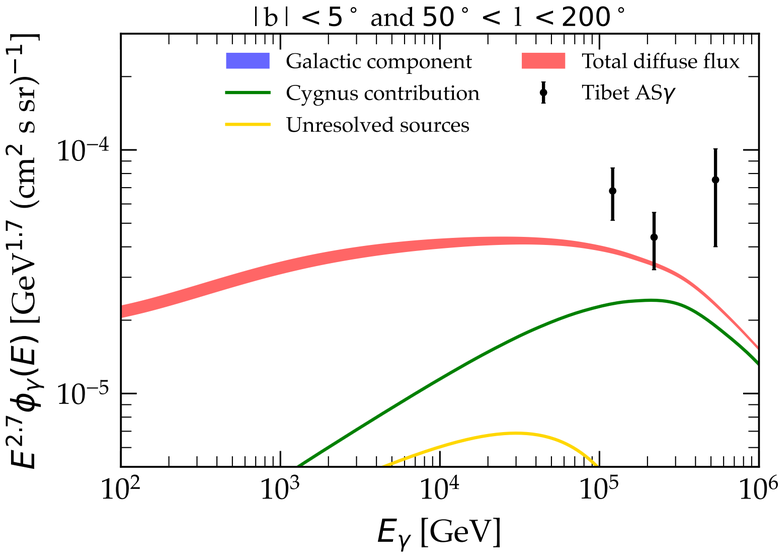
LHAASO





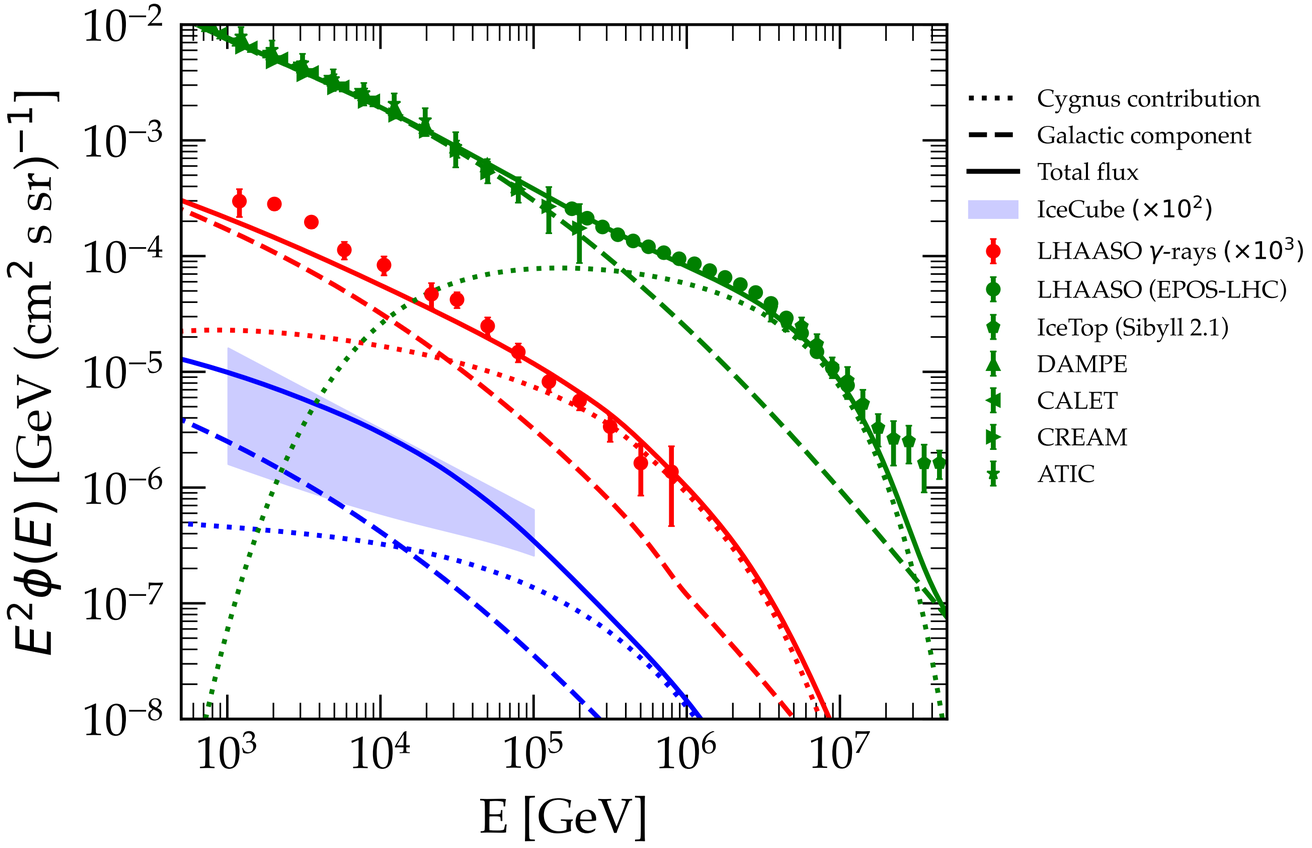
Tibet ASγ





Results and Outlook

For more details see **arXiv: 2603.21665**



Results

A two-population model (with local source in the Cygnus region) is able to:

- Account for a dominant contribution at the knee.
- Reproduce spectral and spatial observations of the VHE diffuse gamma-rays.
- Imply a neutrino emission compatible with IceCube observations.

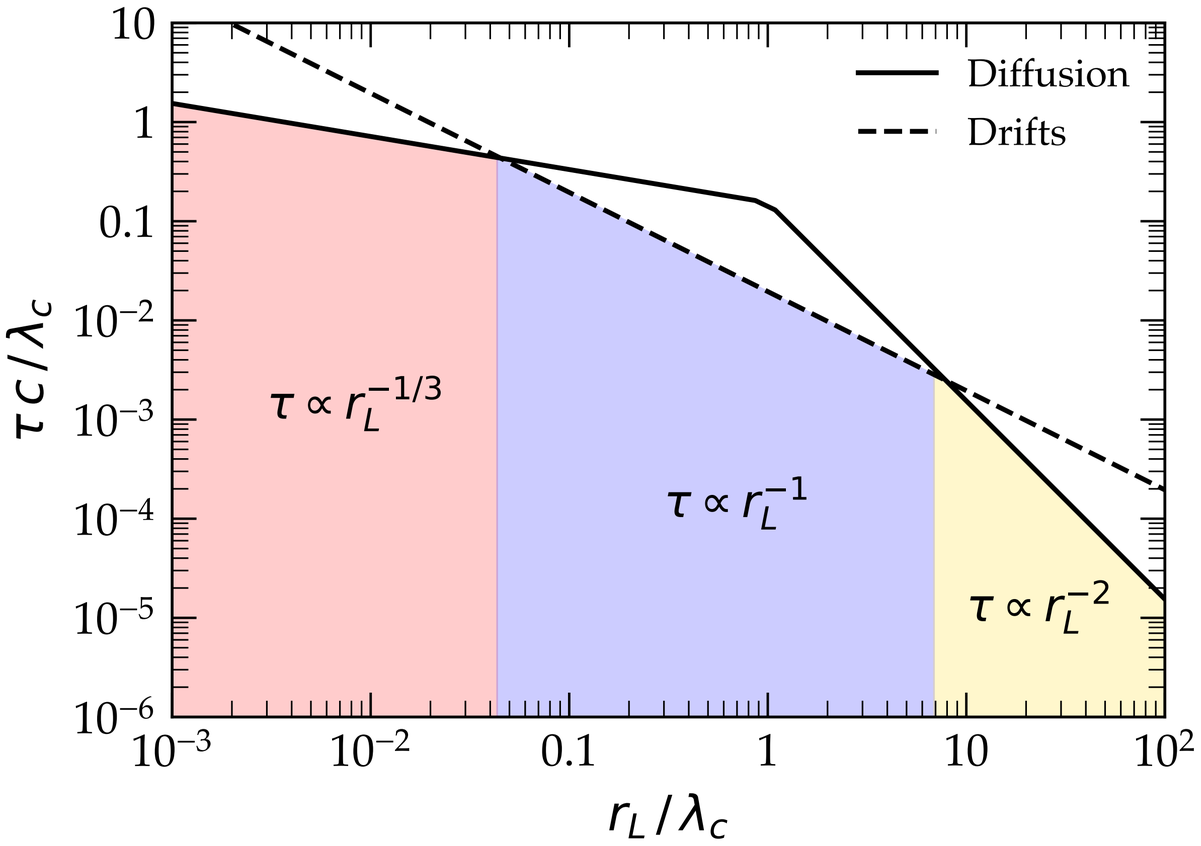
Outlook

- Identification of source properties to distinguish the accelerator type (microquasars, YMSC, hypernova, etc).
- Estimate cumulative contribution of these sources.
  - ⋆ How likely is that a local source dominates the cosmic ray flux?
  - ⋆ How many of these sources do we expect to be active in the Galaxy?

The ‘Transport’ Scenario

Diffusion-Drift Transition as the Origin of the Knee

In the presence of a regular field with variations (such as large-scale gradients and curvatures) on scales larger than the Larmor radius, **drifts** arise in direction perpendicular to both the coherent field and spatial variation **[Isenberg+1979]**.



For realistic turbulence levels $\left(\delta B/B_0\right)$ in the Galaxy, drifts may dominate at high energies, producing a knee-like spectral break **[Ptuskin+1993]**.

Spectral break is expected to involve a change of spectral index $\Delta\gamma \sim 0.5 - 0.7$ **[Candia+2003]**.

- Can a diffusion-drift transition occur at PeV energies?
- Does the resulting confinement times are in agreement with the expected accumulated cosmic ray grammage?

Test-Particle Simulations in Synthetic Fields

Galactic Magnetic Field

- Toroidal coherent field

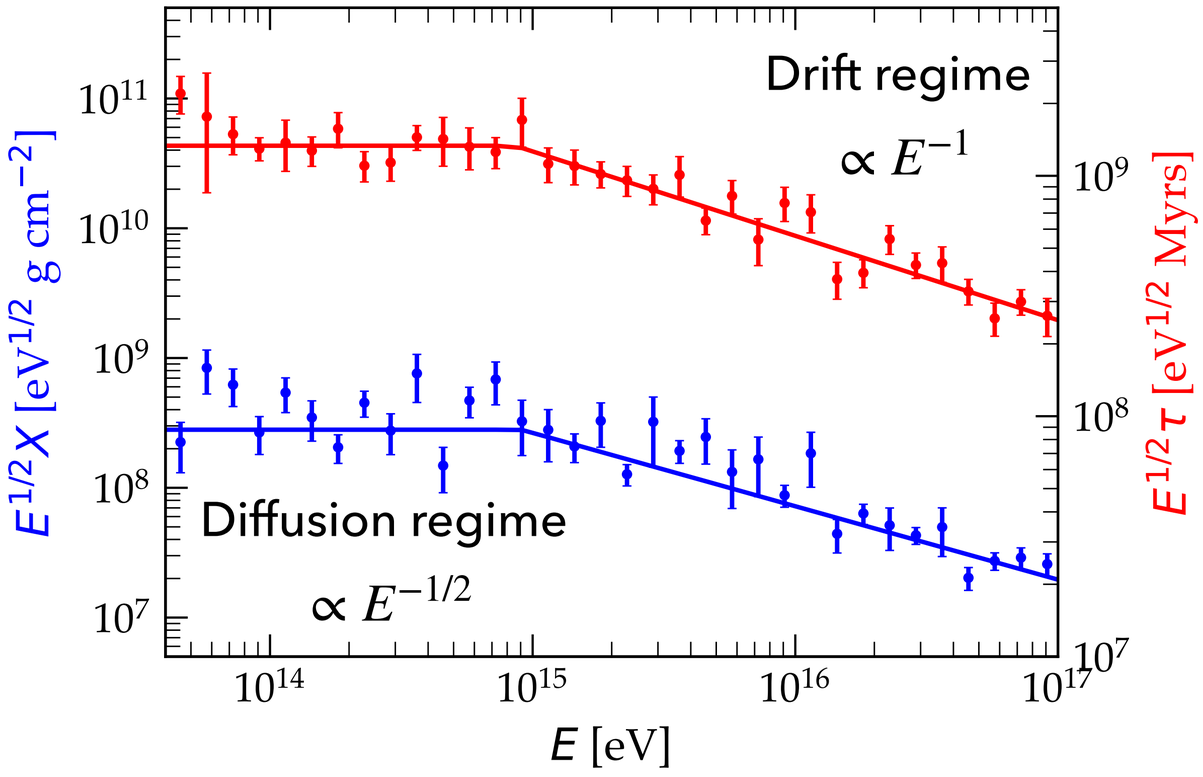
$$B_0^2(x,y,z) = \begin{pmatrix} (1-\mu)B_0^2 \dfrac{y^2}{x^2+y^2} \\ -(1-\mu)B_0^2 \dfrac{x^2}{x^2+y^2} \\ \mu B_0^2 \end{pmatrix}$$

- Antisymmetric with respect to Galactic plane, $B_\phi(z) = -B_\phi(-z)$ **[Unger+2024, Krause+1980].**

- Turbulent component: isotropic, homogeneous, with Kolmogorov spectrum and turbulence level $\eta = \delta B/B_0 < 1$.

CRPropa

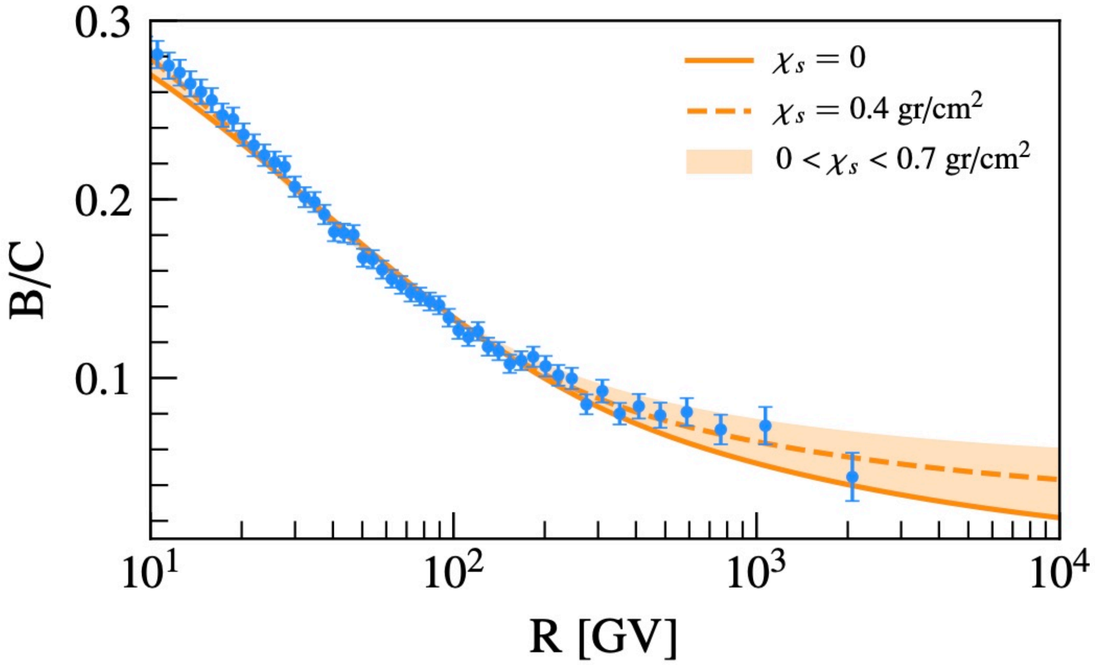
We perform simulations in CRPropa 3.2 **[Alves Batista+2022]** of cosmic rays propagating in a Galactic box, tracking their positions, to compute their confinement time and accumulated grammage before reaching halo height $H = 2$ kpc.



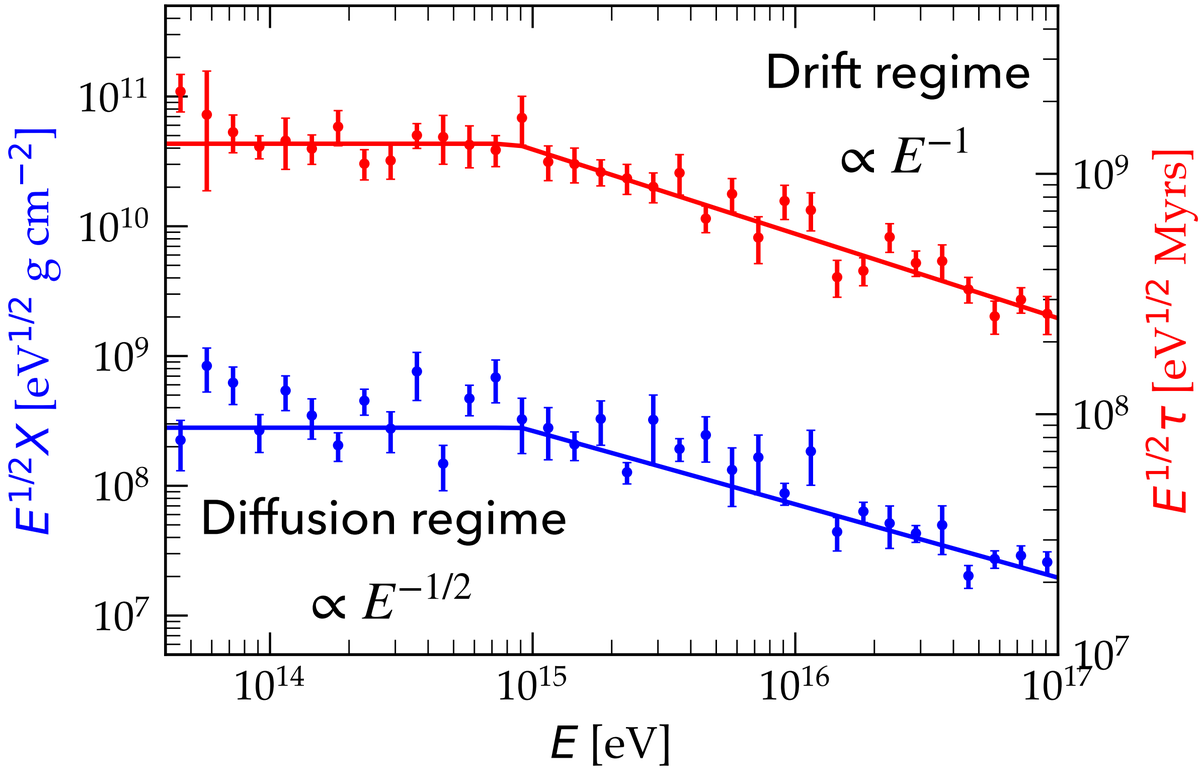
Test-Particle Simulations in Synthetic Fields

Grammage at TeV inferred from direct observations $\sim 0.6\,\mathrm{g\,cm^{-2}}$.

Perpendicular diffusion is an **inefficient mechanism** for particle escape, produces residence times and grammage about two orders of magnitude greater.



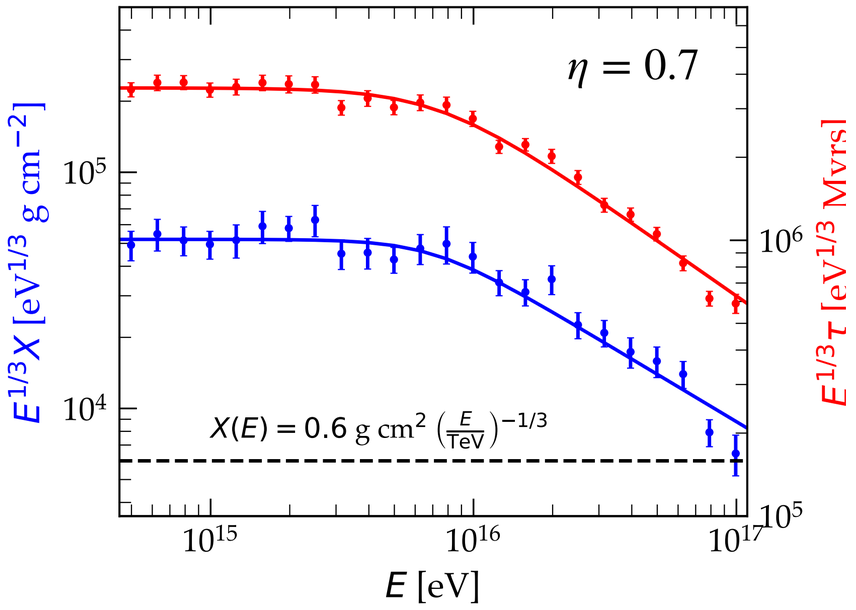
We perform simulations in CRPropa 3.2 **[Alves Batista+2022]** of cosmic rays propagating in a Galactic box, tracking their positions, to compute their confinement time and accumulated grammage before reaching halo height $H = 2$ kpc.

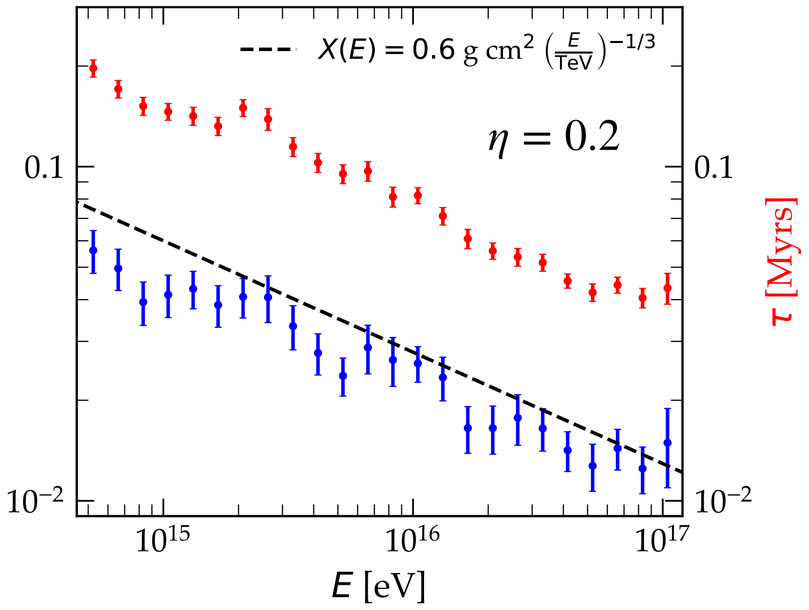


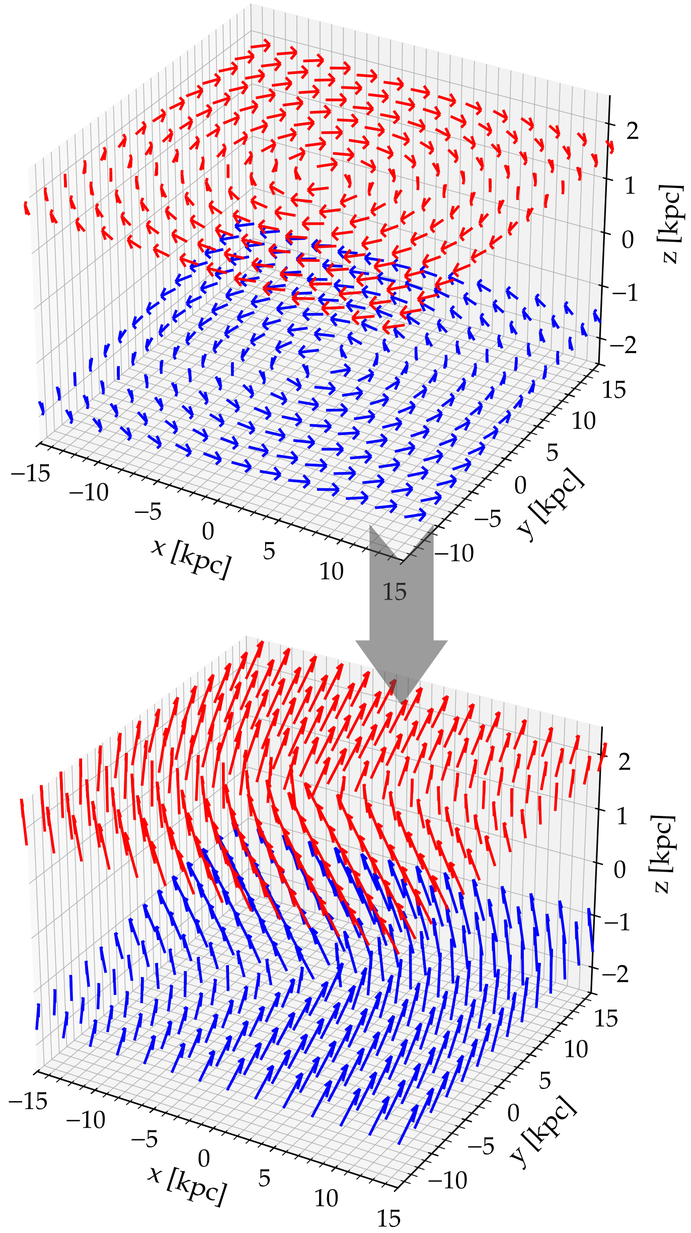
Test-Particle Simulations in Synthetic Fields

Enhancement of particle escape possible if a **vertical component of the large scale magnetic field** is introduced, situation reminiscent of the presence of winds.

At low turbulence, **parallel diffusion dominates** cosmic ray transport over perpendicular diffusion and drifts, removing the ‘knee-like’ break.







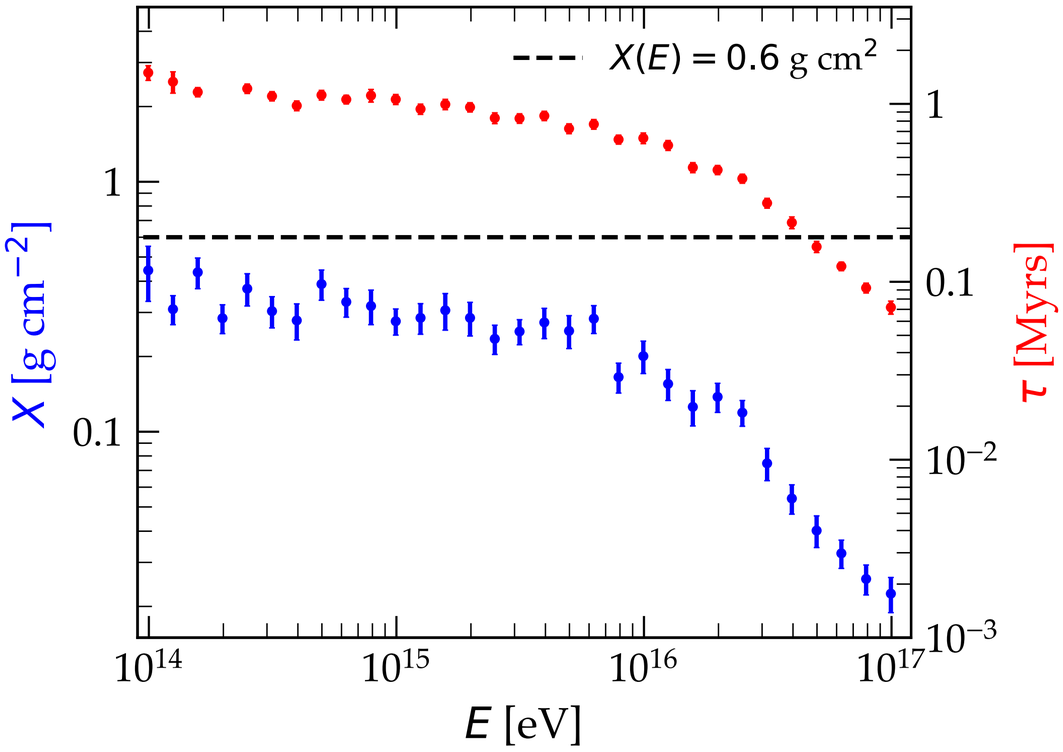
The Case of Energy-Independent Diffusion Coefficient

- Recent MHD simulations show roughly energy-independent diffusion, either due to lack of resonant plasma modes or via scattering with intermittencies **[Kempski+2025, Puzzoni+2026]**.

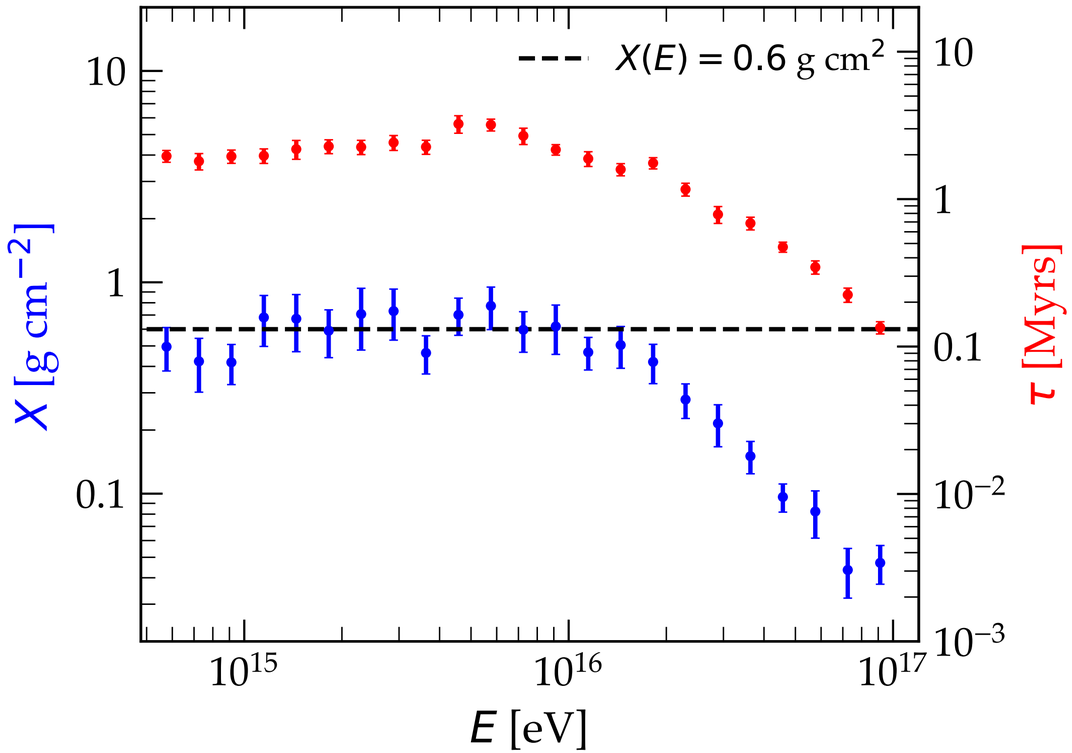
- Flattening of B/C can be connected to energy-independent transport **[Recchia+2024]**.

Energy-independent diffusion could be obtained synthetically via magnetic power spectra:

$W(k) \propto k^{-2}$



$W(k) \propto \delta\left(k \sim 1/\lambda_c\right)$ for $\eta > 1$ **[Pezzi+2023]**



Results and Outlook

Results

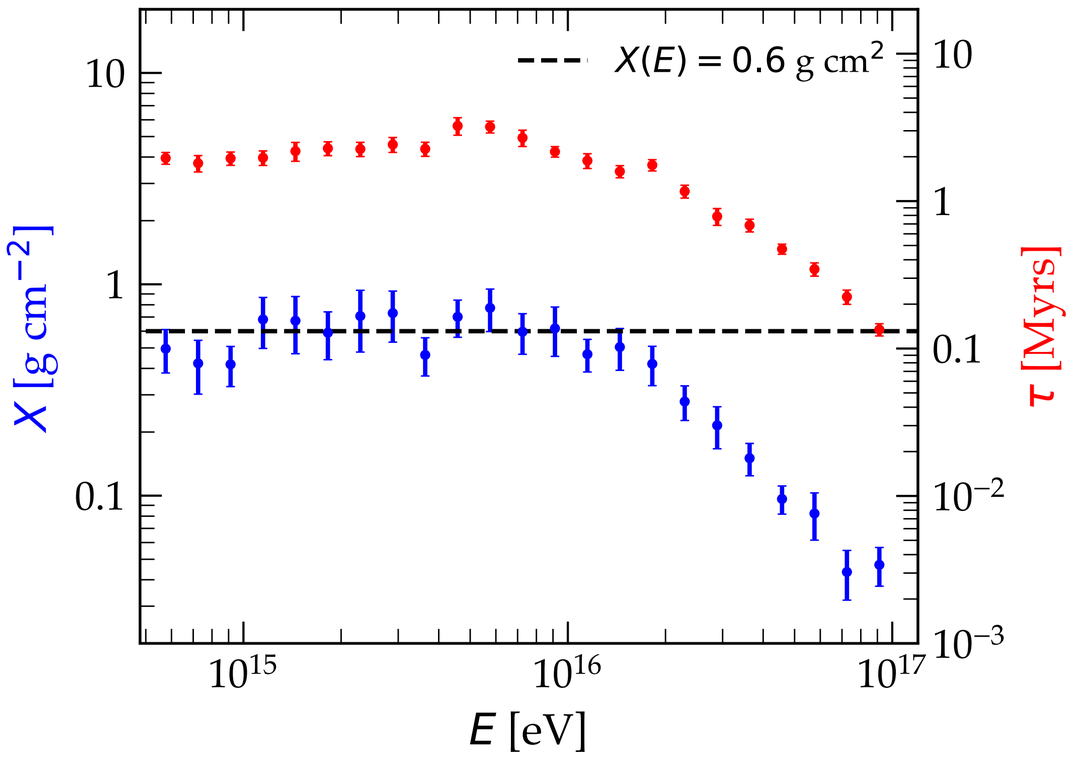
The diffusion-drift transition model:

- Predicts a **spectral break** that resembles the cosmic ray knee.
- Is difficult to reconcile with observations of **cosmic ray grammage**.
- Requires **non-standard transport** of particles from TeV to PeV energies.

Outlook

- What is the implication on other observables, namely radioactive isotopes?
- What is the impact of spatial-dependent variations of the coherent magnetic field, e.g. $\mu(R, z)$?
- How ‘flat’ diffusion truly is at the TeV range?

For more details see **arXiv: 2606.28141**



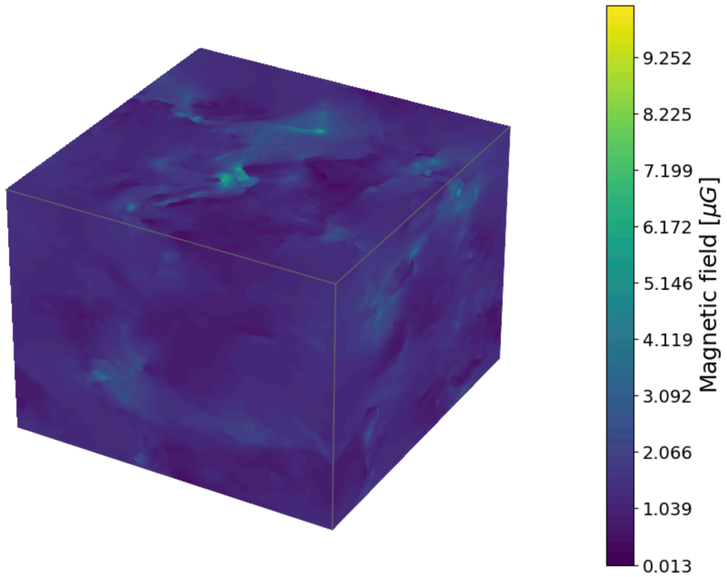
MHD Turbulence

Simulations of MHD Turbulence

- Simulations performed with RAMSES, an adaptive mesh refinement ideal-MHD code.
- Turbulence is injected at $t = 0$ by considering an external forcing on the MHD equations:

$$\frac{\partial}{\partial t}(\rho\vec{v}) + \nabla \cdot (\rho\,\vec{v} \times \vec{v}) + \nabla P = -\,\rho\,\nabla\phi + \rho\,\overrightarrow{F}$$

$$\frac{\partial}{\partial t}(\rho e) + \nabla \cdot (\rho\vec{v}[e + P/\rho]) = -\,\rho\vec{v} \cdot \nabla\phi + \rho\,\overrightarrow{F} \cdot \vec{v}$$



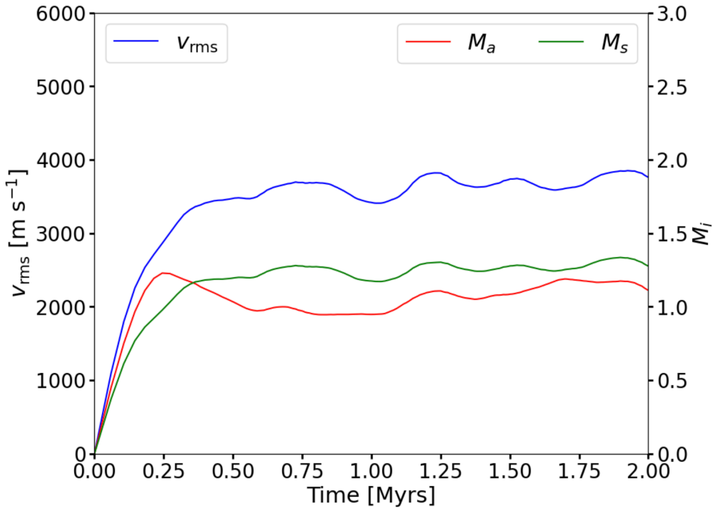
$$d\overrightarrow{F}\left(\vec{k},t\right) = F_0\left(\vec{k}\right)\overrightarrow{P}\left(k_x,k_y,0\right)d\overrightarrow{W_t} - \overrightarrow{F}\left(\vec{k},t\right)\frac{dt}{T}$$

with injection spectrum $F_0\left(\vec{k}\right) = 1 - \left(|k| - k_0\right)^2$

$$\text{for } k_0 = \frac{2\pi}{L_{\text{inj}}}$$

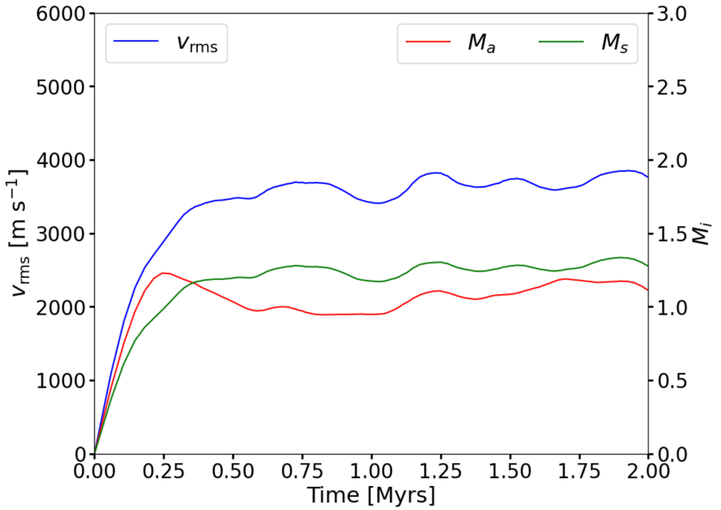
Development of turbulence

One can study the time evolution of turbulence, the resulting cascading process as well as change the conditions of injection.



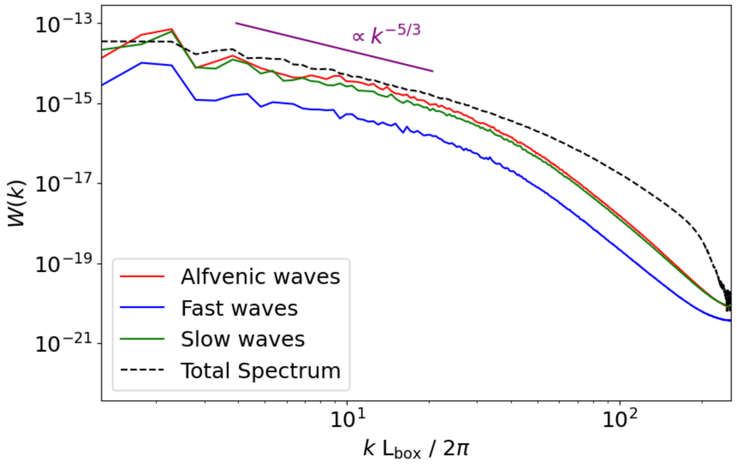
Development of turbulence

One can study the time evolution of turbulence, the resulting cascading process as well as change the conditions of injection.



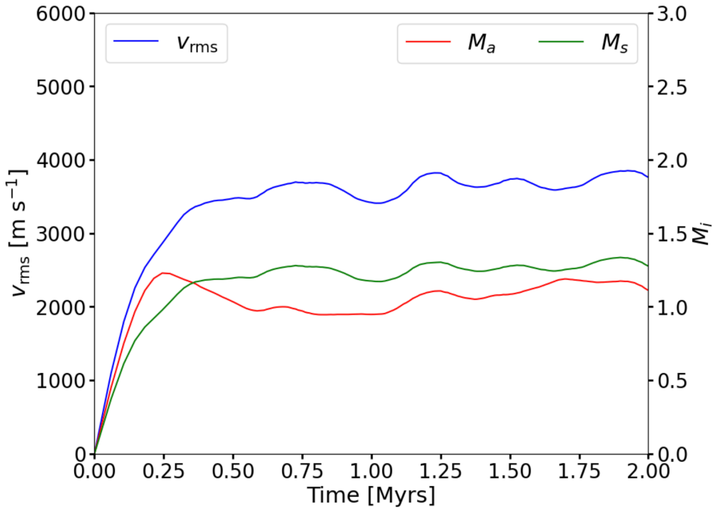
Plasma waves

The resulting fields can be decomposed in plasma modes (Alfvénic and magnetosonic) to identify differences in spectrum.



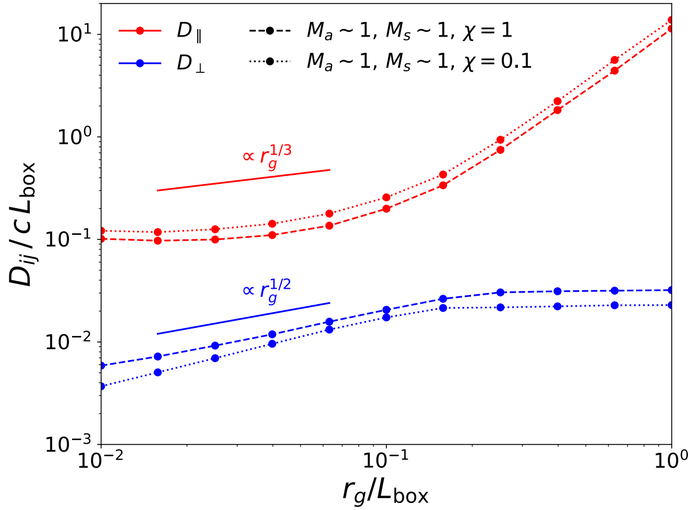
Development of turbulence

One can study the time evolution of turbulence, the resulting cascading process as well as change the conditions of injection.



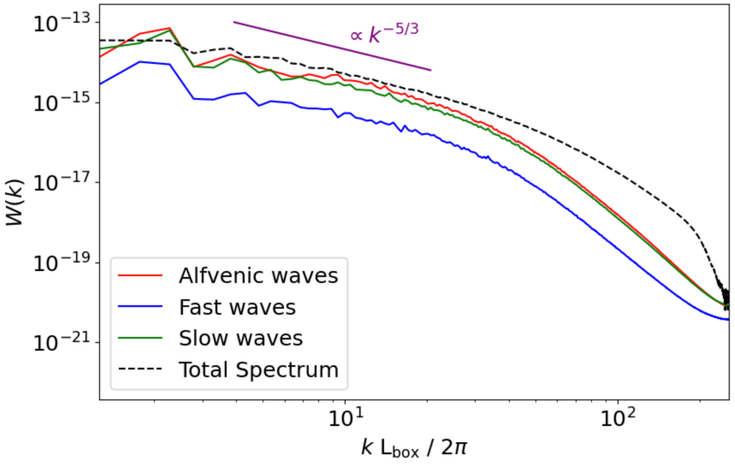
Test-particle simulations

For sufficiently highly-resolved boxes, particle diffusion can be measured as function of turbulence regime and energy.



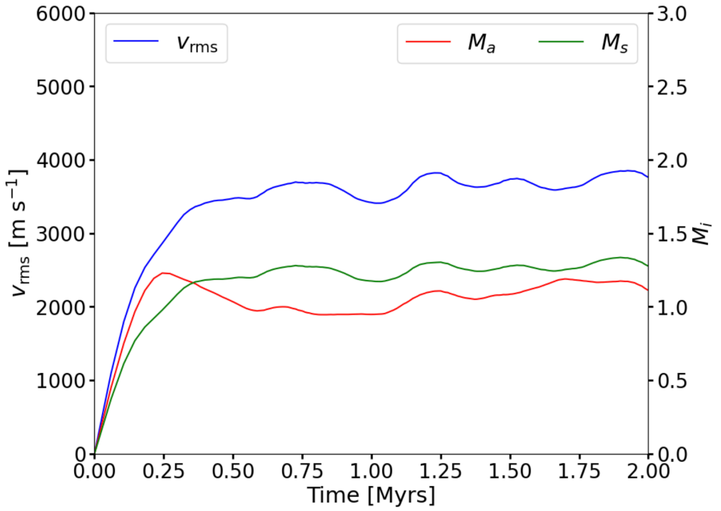
Plasma waves

The resulting fields can be decomposed in plasma modes (Alfvénic and magnetosonic) to identify differences in spectrum.



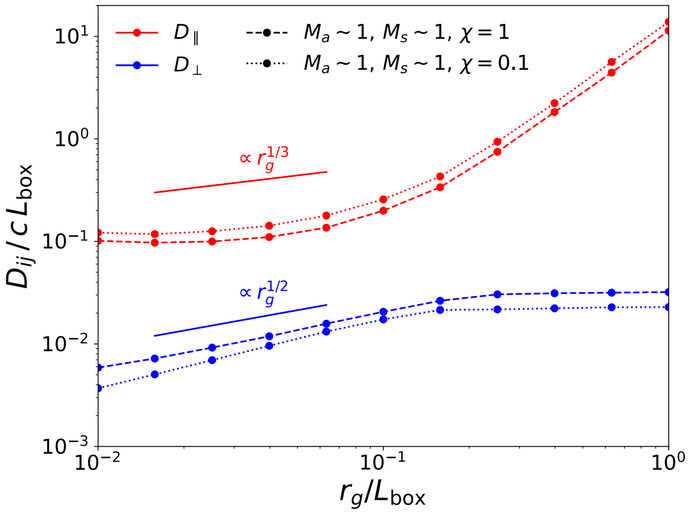
Development of turbulence

One can study the time evolution of turbulence, the resulting cascading process as well as change the conditions of injection.



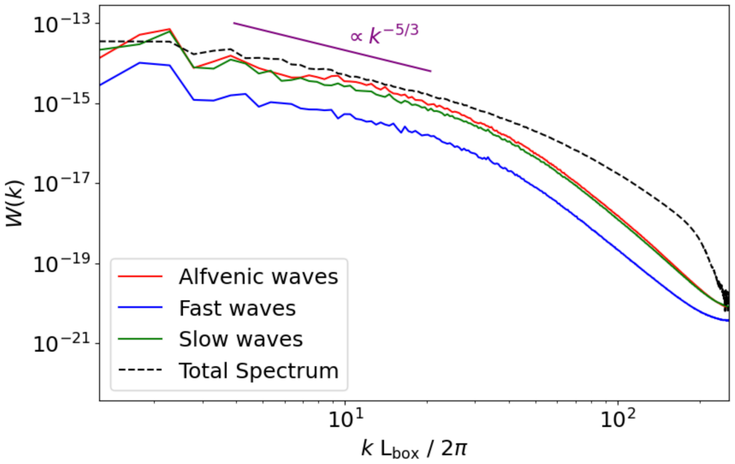
Test-particle simulations

For sufficiently highly-resolved boxes, particle diffusion can be measured as function of turbulence regime and energy.



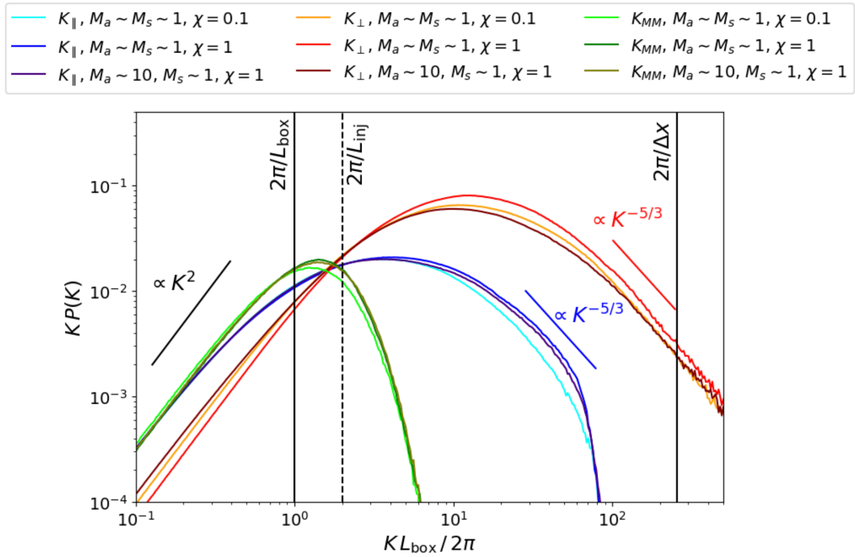
Plasma waves

The resulting fields can be decomposed in plasma modes (Alfvénic and magnetosonic) to identify differences in spectrum.



Magnetic structures

The statistics of field-line intermittent structures can be extracted to evaluate their role on particle diffusion.



Summary

- The two classes of solutions (**sources and transport**) for the origin of the cosmic ray knee have been explored.
- For both cases, it is require to go beyond the standard picture for a satisfactory reproduction of this feature and other observables (grammage, confinement time, gamma-rays and neutrinos).
- For the **source scenario:**
    - A separation between a global population and a ‘PeVatron’ population is required.
    - PeVatrons should be rare (possibly young) sources in the Galaxy.
- For the **transport scenario:**
    - The large scale magnetic field geometry should favour parallel diffusion.
    - Diffusion in intrinsic turbulence should be roughly energy-independent.

- Both solutions are not independent, in fact they are strongly correlated.
- Further observations may be able to distinguish between both models and clarify the physics of the cosmic ray transition.

Publications

- L. E. Espinosa Castro, et al., MNRAS Lett., 543, (2025)
- **L. E. Espinosa Castro, C. Evoli and P. Blasi, Phys. Rev. D 114, (2026)**
- **L. E. Espinosa Castro, et al. (2026), arXiv:2603.21665**
- **J. Tissino, et al. (2026), arXiv:2606.04918**
- **L. E. Espinosa Castro, et al., EPJ Web of Conferences (2026)**
- L. E. Espinosa Castro, et al., PoS ICRC2025, 640 (2025)
- L. E. Espinosa Castro, C. Evoli, and P. Blasi, PoS ICRC2025, 037 (2025)
- I. Vaiman, C. Evoli, and L. E. Espinosa Castro, PoS ICRC2025, 148 (2025)

Outreach

- SHARPER (European Research Night September) / Street Science - September 2024; L'Aquila, Italy
- SHARPER (European Research Night September) / Street Science - September 2025; L'Aquila, Italy
- Guide for Laboratori Nazionali del Gran Sasso

Conferences and Workshops

- 39th International Cosmic Ray Conference - July 2025; Geneva, Switzerland
- Toulouse, Arcetri, and L'Aquila Retreat - October 2025; Arcetri, Italy
- **TeV Particle Astrophysics Conference 2025 - November 2025; Valencia, Spain**
- **Kinetic Physics of Astrophysical Plasmas Workshop - May 2026; Montpellier, France**
- **29th European Cosmic Ray Symposium - July 2026; Santiago de Compostela, Spain**
- **23rd International Symposium on Very High Energy Cosmic Ray Interactions - July 2026; Lecce, Italy**
- **14th Cosmic-Ray International Studies and Multi-messenger Astroparticle Conference - July 2026; Sorrento, Italy**
- **TeV Particle Astrophysics Conference 2026 - September 2026; Tendo, Japan**
- **3rd Cosmic Rays `a l'Observatoire de la Cˆote d'Azur Workshop - September 2026; Nice, France**